blood RCI
red cells & iron

American Society of Hematology
2021 L Street NW, Suite 900,
Washington, DC 20036
Phone: 202-776-0544 | Fax 202-776-0545
bloodrci@hematology.org

Itaconate promotes the differentiation of murine stress erythroid progenitors by increasing Nrf2 activity

Tracking no: RCI-2025-000105-T

Robert Paulson (Penn State University, United States) Baiye Ruan (Regeneron Pharaceuticals, United States) Yuanting Chen (Merck Pharmaceuticals, United States) Sara Trimidal (Penn State University, United States) Meghna Chakraborty (Penn State University, United States) Aashka Shah (Penn State University, United States) Hangdi Gong (Penn State University, United States) Imhoi Koo (Penn State University, United States) Jingwei Cai (Penn State University, United States) John McGuigan (Penn State University, United States) Molly Hall (Penn State University, United States) Andrew Patterson (Penn State University, United States) K. Sandeep Prabhu (The Pennsylvania State University, United States)

Abstract:
Steady state erythropoiesis produces new erythrocytes at a constant rate to replace senescent erythrocytes removed in the spleen and liver. Inflammation caused by infection or tissue damage skews bone marrow hematopoiesis, increasing myelopoiesis at the expense of steady state erythropoiesis. To compensate for the loss of production, stress erythropoiesis is induced. Stress erythropoiesis is highly conserved between mouse and human. It utilizes a strategy different than the constant production of steady state erythropoiesis. Inflammatory signals promote the proliferation of immature stress erythroid progenitors (SEPs), which then commit to differentiation. This transition relies on signals made by niche macrophages in response to erythropoietin. Nitric oxide dependent signaling drives the proliferation of stress erythroid progenitors and production of nitric oxide must be decreased so that the progenitor cells can differentiate. Here we show that as progenitor cells transition to differentiation, increased production of the anti-inflammatory metabolite itaconate activates Nfe2l2 or Nrf2, which decreases Nos2 expression, leading to decreased nitric oxide production. Mutation of Irg1, the enzyme that catalyzes the production of itaconate, causes a delayed recovery from inflammatory anemia induced by heat killed Brucella abortus. These data show that the differentiation of stress erythroid progenitors relies on a switch to an anti-inflammatory metabolism and increased expression of pro-resolving cytokines.

Conflict of interest: No COI declared

COI notes:

Preprint server: Yes; Biorxiv doi: https://doi.org/10.1101/2023.03.11.532211

Author contributions and disclosures: B.R., K.S.P and R.F.P. conceived and designed the study. B.R., S.T., M.C., AS, H.G. and Y.C. performed the experiments. B.R., J.M., and M.A.H. analyzed the RNA-seq data. B.R., I.K., J.C., and A.D.P. analyzed the metabolomics analysis. B.R. and R.F.P. wrote the initial draft of the manuscript, and all authors were involved in review and editing.

Non-author contributions and disclosures: No;

Agreement to Share Publication-Related Data and Data Sharing Statement: For original Data please contact rfp5@psu.edu RNA-sequencing data have been deposited at NCBI GEO with accession number GSE190030. Metabolomics data have been deposited at NMDR (DOI: http://dx.doi.org/10.21228/M89402).

Clinical trial registration information (if any):

Itaconate promotes the differentiation of murine stress erythroid progenitors by increasing Nrf2 activity.

Baiye Ruan[1,3], Yuanting Chen[2,3], Sara Trimidal[6], Meghna Chakraborty[6], Aashka Shah[6], Hangdi Gong[2], Imhoi Koo[3], Jingwei Cai[3], John Mcguigan[3], Molly A. Hall[3,5,] Andrew D. Patterson[3,5], K. Sandeep Prabhu[1-5], Robert F. Paulson[1-7]

[1]Graduate Program in Pathobiology, [2]Graduate Program in Molecular, Cellular and Integrative Bioscience, [3]Department of Veterinary and Biomedical Sciences, [4]Center for Molecular Immunology and Infectious Disease, [5]Center for Molecular Toxicology and Carcinogenesis, [6]Graduate Program in Biochemistry, Microbiology and Molecular Biology, Pennsylvania State University, University Park, PA 16802, USA

[7]Corresponding Author:
Robert F. Paulson, PhD
Address: 203 AVBS Building, 439 Shortlidge Road, University Park, PA 16802, USA
Email: rfp5@psu.edu
Phone: 814-863-6306

For original data contact rfp5@psu.edu
RNA-sequencing data have been deposited at NCBI GEO with accession number GSE190030.
Metabolomics data have been deposited at NMDR (DOI: http://dx.doi.org/10.21228/M89402).

Short title: Itaconate promotes stress erythropoiesis.

Word count for text: 3991

Word count for abstract: 207

Figure count: 7

Reference count: 50

Supplemental Data: Methods + 3 Tables + 6 Figures

31

Key points

1. Anti-inflammatory signals promote the transition to differentiation of stress erythroid progenitors.

2. The anti-inflammatory metabolite itaconate increases Nrf2 activity to promote the differentiation of stress erythroid progenitors.

Abstract

Steady state erythropoiesis produces new erythrocytes at a constant rate to replace senescent erythrocytes removed in the spleen and liver. Inflammation caused by infection or tissue damage skews bone marrow hematopoiesis, increasing myelopoiesis at the expense of steady state erythropoiesis. To compensate for the loss of production, stress erythropoiesis is induced. Stress erythropoiesis is highly conserved between mouse and human. It utilizes a strategy different than the constant production of steady state erythropoiesis. Inflammatory signals promote the proliferation of immature stress erythroid progenitors (SEPs), which then commit to differentiation. This transition relies on signals made by niche macrophages in response to erythropoietin. Nitric oxide dependent signaling drives the proliferation of stress erythroid progenitors and production of nitric oxide must be decreased so that the progenitor cells can differentiate. Here we show that as progenitor cells transition to differentiation, increased production of the anti-inflammatory metabolite itaconate activates Nfe2l2 or Nrf2, which decreases Nos2 expression, leading to decreased nitric oxide production. Mutation of Irg1, the enzyme that catalyzes the production of itaconate, causes a delayed recovery from inflammatory anemia induced by heat killed *Brucella abortus*. These data show that the differentiation of stress erythroid progenitors relies on a switch to an anti-inflammatory metabolism and increased expression of pro-resolving cytokines.

Introduction

Steady state erythropoiesis constantly produces new erythrocytes at a rate of 2.5x10^6 per second[1]. Senescent or damaged erythrocytes are removed from circulation by macrophages in the spleen and liver at a similar rate, which maintains erythroid homeostasis[2]. In contrast, pro-inflammatory signals alter the kinetics and routes of hematopoietic differentiation leading to increased production of myeloid cells at the expense of steady state erythropoiesis[3-8]. Additionally, inflammation increases erythrophagocytosis which shortens the life span of erythrocytes and increases iron sequestration, which limits hemoglobin synthesis[9-12]. These demand-adapted changes in the blood system underpin a protective immune response to inflammatory insults, but they come with a cost as steady-state erythropoiesis is compromised. Given that effective oxygen transport requires adequate levels of erythrocytes, a compensatory stress erythropoiesis response is activated that utilizes inflammatory signals to produce erythrocytes and maintain homeostasis during inflammation[13].

Stress erythropoiesis utilizes a different strategy than steady state erythropoiesis. Inflammation induces the migration of short-term hematopoietic stem cells (CD34+Kit+Sca1+) and monocytes to the spleen[14-16]. Pro-inflammatory signals like tumor necrosis factor-α (TNFα), interleukin 1β (IL-1β) and interferon γ (Ifnγ) in combination with SCF, canonical Wnt signaling, hedgehog and Growth and differentiation factor 15 (GDF15) promote the proliferation of a transient amplifying population of stress erythroid progenitors (SEPs)[17-22]. These signals also establish a stress erythropoiesis niche[15, 18]. The expansion of this population of immature SEPs and the development of the niche marks the initial stage of stress erythropoiesis. The transition of this population of SEPs from proliferating SEPs to SEPs committed to erythroid differentiation is driven be erythropoietin (Epo) dependent changes in niche signals[18]. Pro-inflammatory and proliferation promoting signals are turned off and pro-differentiation signals like Prostaglandin E2 promote the transition to SEPs committed to differentiation. Overall, this

transition relies on a switch from pro-inflammatory signals to pro-resolving signals. This change in signals is like that observed when macrophages promote the resolution of inflammation by increasing the expression of IL-4, IL-10 and the anti-inflammatory metabolite itaconate[23, 24].

The tight spatiotemporal coordination between niche cells and SEPs suggest that they may utilize the same immunomodulatory molecules to regulate their co-development. Whereas the role of these molecules in macrophages is extensively studied, it remains undetermined how immunoregulatory metabolites and cytokines act on SEPs to affect their development. In this study, we applied integrated analysis of transcriptional and metabolic profiling on SEPs at different developmental stages. We show that transition of SEPs from expansion to differentiation is dependent on a switch of progenitor cell signaling from one dominated by inflammatory signals to one dominated by resolving signals. In the expansion stage, Nitric oxide synthase 2 (Nos2)-dependent nitric oxide (NO) production drives the proliferation of immature SEPs (Ruan et al. bioRxiv[25], unpublished data). In contrast, the transition to SEP differentiation is marked by decreased inflammatory signals and increased resolving molecules like itaconate. The anti-inflammatory effects of itaconate is mediated by the nuclear factor erythroid 2-related factor 2 (Nfe2l2 or Nrf2). Activation of Nrf2 resolves inflammatory signals in both SEPs and the niche, which reduces NO levels and alleviates the NO-mediated erythroid inhibition. These data provide a mechanistic basis of how SEP cell-fate transition is governed by immunomodulatory molecules to ensure effective erythroid regeneration.

Methods

Mice

Wild-type C57BL/6J, B6.SJL-Ptprca Pepcb/BoyJ (CD45.1) JAX stock #002014, B6.129X1-Nfe2l2tm1Ywk/J (Nrf2-/-) JAX stock #017009[26], B6.129P2-*Il10*^{tm1Cgn}/J (IL-10-/-) JAX stock# 002251[27] and C57BL/6N-Acod1em1(IMPC)J/J (Irg1-/-) JAX stock #029340 mice were purchased from Jackson Laboratories. Mice of both sexes at age 8-16 weeks were used throughout this study. All experiments were approved by the Institutional Animal Care and Use Committee (IACUC) at the Pennsylvania State University.

Stress erythropoiesis in vitro cultures

Mouse stress erythropoiesis cultures were done as previously described[16]. Details of the media and culture conditions are provided in the supplementary data.

In vivo induction of stress erythropoiesis

Phenylhydrazine (PHZ) was used to induce stress erythropoiesis in the context of acute hemolytic anemia. Mice were injected intraperitoneally with a single dose (100 mg/kg body weight) of freshly prepared phenylhydrazine (Sigma-Aldrich, dissolved in PBS)[28]. Heat-killed Brucella abortus (HKBA, strain 1119-3) was used to induce anemia of inflammation according to a previously described method[29].

Stress BFU-E colony assay[28]

SEPs isolated from stress erythropoiesis differentiation media (SEDM) cultures or mouse splenocytes were counted using a hemocytometer. For each sample, 2.5 x 10^5 cells were resuspended in 2 ml MethoCult M3334 media (STEMCELL Technologies) supplemented additionally with 50 ng/ml SCF (GoldBio) and 15 ng/ml BMP4 (Thermo Fisher Scientific), and cell suspension was evenly plated into 3 wells of a 12-well plate as technical triplicates. Stress BFU-E colonies were stained with benzidine and quantified after a 5-day culture in 37 °C with 2% O_2 and 5% CO_2.

Statistics

GraphPad Prism and R were used for statistical analysis. Statistical significance between two groups was determined by two-tailed unpaired t test, except for the human culture experiment where paired t test was performed. Data with more than two groups were assessed for significance using one-way or two-way ANOVA followed by specific post hoc test as noted in the figure legends. Tukey's test was used to make every possible pairwise comparison, whereas Dunnett's correction was used to compare every group to a single control. Hematocrit levels were measured at different time points from same cohorts of mice, and data were analyzed by two-way repeated measures ANOVA followed by unpaired t test. Data are presented as mean ± SEM. Less than 0.05 of p value is considered as significant difference. n.s., $p > 0.05$; *, $p < 0.05$; **, $p < 0.01$; ***, $p < 0.001$.

Data sharing statement

RNA-sequencing data have been deposited at NCBI GEO with accession number GSE190030. Metabolomics data have been deposited at NMDR (DOI: http://dx.doi.org/10.21228/M89402).

Additional methods are available in supplemental methods.

Results

Itaconate production increases during the transition from SEP proliferation to differentiation.

Our previous work showed that the commitment of SEPs to erythroid differentiation is driven by changes in the signals made by the niche. Pro-inflammatory signals like TNFα, IL-1β and Wnt factors promote proliferation, but their expression is decreased during the commitment to differentiation, and they are replaced by pro-resolving signals like prostaglandin E2 and Prostaglandin J2[17, 18]. We hypothesized that metabolites generated by these signals could contribute to the regulation of cell proliferation and differentiation. We performed LC-MS

analysis to profile the changes of metabolites extracted from bulk SEPs on days 1 and 3 of stress erythropoiesis expansion media (SEEM) cultures, when pro-inflammatory signals are driving proliferation of SEPs. We observed that the endogenous pro-resolving metabolite itaconate decreased significantly from day 1 to day 3 of SEEM culture, which corresponds to the start of SEP proliferation (Figure 1A). Further analysis of itaconate levels in SEPs on day 3 and 5 during expansion culture compared with days 1, 2 and 3 of stress erythropoiesis differentiation media (SEDM) culture showed that itaconate increases at day 5 of expansion, which correlates with increase in stress BFU-E and peaks at day 1 of differentiation and is maintained at that level through day 3 (Figure 1B)[16]. Immunoresponsive gene 1 (*Irg1*) encodes the enzyme that catalyzes itaconate synthesis by the decarboxylation of cis-aconitate[30]. Analysis of *Irg1* mRNA and protein showed that in Kit+SEPs, mRNA increases from SEEM day 3 to day 5 and then decreases after the cultures are placed in SEDM. In contrast the protein levels increase at SEDM day1 and are maintained at Day 5 (Figure 1C and S1A). We observed similar Irg1 mRNA and protein expression levels in the stromal cells of the culture.

Itaconate inhibits NO dependent proliferation.

Itaconate is an anti-inflammatory mediator[31] and the levels of itaconate were lower when SEPs were proliferating and increased during the transition to differentiation. NO dependent signaling promotes the proliferation of SEPs and inhibits their differentiation (Ruan et al. BioRxv[25] unpublished data). We hypothesized that treating cells with a cell permeable form, 4-octyl-itaconate (OI)[30, 32], could decrease the pro-inflammatory signaling that drives the expansion of SEP progenitor populations. OI impaired SEP expansion (Figure 2A). In fact, if OI was added at the start of culture, SEPs failed to proliferate. OI-treated SEEM cultures displayed fewer more rapidly proliferating late-stage $Kit^{+}Sca1^{+}CD34^{-}CD133^{+}$ and $Kit^{+}Sca1^{+}CD34^{-}CD133^{-}$ SEPs, while the numbers of the most immature $Kit^{+}Sca1^{+}CD34^{+}CD133^{+}$ progenitors were not affected (Figure 2B-C and S1B). Treatment with OI decreased the mean fluorescent intensity

(MFI) of NO in SEPs including immature Kit+Sca1+ $CD34^{+}CD133^{+}$ progenitors whose numbers were not decreased by OI treatment, which suggests that different progenitors have different requirements for NO (Figure 2D). Our analysis showed that OI reduced the levels of *Nos2* mRNA in SEPs, but the levels of Nos2+SEPs as measured by flow cytometry was not significantly affected (Figure 2E and S1C). However, Nos2+ stromal cells were decreased by OI treatment (Figure 2F). Conversely, the defects in SEP proliferation induced by OI treatment were rescued by treatment with the NO donor SNAP[33] at either 10 or 50 μM, indicating that itaconate impairs proliferation by decreasing NO levels (Figure 2G). We observed the opposite when we cultured Irg1-/- cells as mutation of Irg1 accelerated the transition to more mature $Kit^{+}Sca1^{+}CD34^{-}CD133^{-}$ cells, while Nos2 mRNA expression increased (Figure 2H). As shown above, Nos2 is expressed both in the SEPs and the stromal cells. Nos2 function is not cell autonomous as NO generated by stromal cells rescues Nos2-/- SEPs (Ruan et al. bioRxiv[25], unpublished data). In contrast, Irg1 function is cell autonomous as Irg1-/- SEPs exhibit a defect even when co-cultured with wildtype stroma (Fig S1D). These data support a specific role for itaconate in SEPs.

Nrf2 is required for itaconate dependent regulation of SEP expansion.

Itaconate alkylates Keap1 and acts as a potent inducer of Nrf2 activity, which is a central regulator of the response to oxidative stress[32]. Nrf2 is also involved in anti-inflammatory response, and this function is essential for the immunomodulatory role of itaconate in the activated macrophages[32]. We hypothesized that itaconate inhibits SEP proliferation by promoting the activation of Nrf2. Similar to what we observed with Irg1-/- mutations, Nrf2-/- SEPs cultured on wildtype stroma exhibited a defect in differentiation that was as severe as Nrf2-/- cultures. However, consistent with work from Gotosho et al., which showed a requirement for Nrf2 signaling in macrophages during stress erythropoiesis, we also observed a smaller defect in differentiation when control SEPs were grown on Nrf2-/- stroma[34]. These data demonstrate a cell autonomous role for Nrf2 in SEPs and a smaller autonomous role in the

stroma (Figure S2A-D). The expression of Nrf2 protein increased in SEPs and the stroma when cells were shifted to SEDM, which was similar to what we observed for Irg1 (Figure 3A and S2E). Nrf2 transcriptional activity as measured by mRNA expression of NAD(P)H:quinone oxidoreductase 1 (*Nqo1*), a direct Nrf2 target showed low levels of expression at day 5 of SEEM culture, but further increased when cells were moved to SEDM (Figure S2F).

Nrf2-deficient SEPs initially grew faster when compared to WT controls, however, there was no difference in total cell numbers at day 5 (Figure 3B). Nrf2-/- cultures contained more late-stage $Kit^{+}Sca1^{+}CD34^{-}CD133^{-}$ progenitors and fewer immature $Kit^{+}Sca1^{+}CD34^{+}CD133^{+}$ SEPs than WT cultures (Figure 3C). While no differences in the number of F4/80+Vcam1+ macrophages in the stroma were observed (Figure S2G)**.** The similarities in expression and phenotypes of Irg1 and Nrf2 mutant progenitors suggests a model where itaconate levels regulate Nrf2 activity, which in turn fine tunes SEP proliferation. To verify this mechanism, WT and Nrf2-/- SEEM cultures were supplemented with OI to increase Nrf2 activity. This treatment increased *Nqo1* mRNA expression in SEPs, which was blocked in Nrf2-/- SEPs (Figure 3D). Furthermore, the defect in SEP proliferation caused by addition of OI was rescued by mutation of Nrf2 in the Nrf2-/- SEPs (Figure 3E). We observed similar response when cultures were treated with dimethyl fumarate (DMF), a second known activator of Nrf2 (Figure S2H-K). These data demonstrate that itaconate increases Nrf2 activity promoting the proliferation of SEPs.

We next examined whether Nrf2 suppresses the inflammatory signals required for SEP expansion. OI treatment decreased expression of *Nos2* mRNA, and this effect was compromised in the Nrf2-/- SEPs (Figure 3F). We further confirmed the role of Nrf2 in regulating SEP proliferation as treatment of SEEM cultures with OI, DMF or another Nrf2 activator tert-Butylhydroquinone (tBHQ)[35] decreased the proliferation of Kit+Sca1+ SEPs (Figure S2L). Our previous data showed that in immature SEPs mRNA expression of *Hif-1α* and *Pdk1* promotes glycolysis, which provides anabolic metabolites for cell proliferation[19]. OI or DMF treatment decreased hypoxia inducible factor 1α (*Hif-1α)* and pyruvate dehydrogenase kinase 1 (*Pdk1)*

mRNA expression in proliferating SEPs and this decrease was reversed by Nrf2 mutation (Figure S3A-B), suggesting that activation of Nrf2 disrupts the inflammatory metabolism required for SEP proliferation.

Itaconate-dependent anti-inflammatory response promotes SEP differentiation.

Previously we showed that Epo signaling in the niche promotes the transition of proliferating progenitors to erythroid differentiation[14, 16, 18]. Gene set enrichment analysis (GSEA) of RNA-seq data from SEPs isolated from stress erythropoiesis cultures switched from SEEM to SEDM showed an enrichment in genes in erythroid pathways in SEDM cultures. While SEPs from SEEM cultures showed enriched expression of genes associated with inflammatory pathways (Figure S4A). The resolution of inflammation was coupled to a profound switch of metabolism, including increased levels of itaconate, which was mirrored by increased protein expression of *Irg1* in Kit+Sca1+ SEPs (Figure 1C and S4B). These data suggest that the transition to differentiation increases the production of itaconate that drives an anti-inflammatory response to promote SEP differentiation. To examine its role in differentiation, we performed SEDM cultures using control or Irg1-/- bone marrow cells in which itaconate production was completely impaired. We restored the levels of itaconate in Irg1-/- cultures with the supplementation of OI. Compared to controls, Irg1-/- SEPs had elevated levels of Nos2 protein and NO production, but treatment with OI decreased Nos2 protein and NO levels to levels comparable to control cells (Figure 4A-C). To test whether itaconate promotes differentiation via NO suppression, we isolated SEPs from control and Irg1-/- SEDM cultures treated with and without the Nos2 specific inhibitor, 1400w[36].Treatment of wildtype SEDM cultures with 1400W leads to increased stress BFU-E and a superinduction of erythroid genes(Ruan et al. bioRxiv[25], unpublished data). Irg1-deficient progenitors generated fewer stress BFU-Es and mature $Kit^{+}Sca1^{-}CD34^{-}CD133^{-}$ SEPs and expressed lower mRNA levels of representative erythroid genes, Erythropoietin receptor (EpoR), Gata1, the heme biosynthetic enzyme, coproporphyrinogen oxidase (Cpox) and beta-major globin (Hbb-b1), indicating that itaconate production is required for the transition to

erythroid differentiation (Figure 4D-F). This defect in differentiation was rescued by treatment with 1400w, a Nos2 specific inhibitor. These data demonstrate that itaconate promotes erythroid differentiation by inhibiting Nos2-dependent NO production.

We next investigated the role of Irg1 *in vivo* during the recovery from Heat Killed *Brucella abortus* (HKBA) induced inflammatory anemia[29, 37, 38]. Untreated Irg1-/- mice exhibited similar levels of SEPs in their spleens and stress BFU-E when compared to wildtype (Figure S5A). Despite this similarity, Irg1-/- mice treated with HKBA exhibited a significant delay in recovery over 28 days (Figure 5A). On day 8 after HKBA treatment, the anemia of control mice starts to improve, and over the next 8 days the mice significantly improve their hematocrit. We examined Irg1-/- and control HKBA treated mice during this critical period in recovery on days 8, 12 and 16. We observed that Irg1-/- mice showed continued decreases in hemoglobin and RBC concentration during this time (Figure 5B). However, this defect of stress erythropoiesis is not due to a lack of SEPs in the spleen as spleen weight and spleen cellularity was increased in the Irg1-/- mice (Figure 5C). The defect is in the differentiation of SEPs. The percentage of $Kit^{+}Sca1^{-}CD34^{-}CD133^{-}$ SEPs was significantly decreased in Irg1-/- mice, while the percentage of Kit+Sca1+$CD34^{+/-}$ CD133+ immature cells increased (Figure 5D-E). This decrease in mature SEPs translated to a lower frequency of stress BFU-E at each time point and fewer overall stress BFU-E on days 8 and 16 (Figure 5F). Analysis of *Nos2* expression in the spleens showed that Irg1-/- mice had increased levels of Nos2 supporting the role for itaconate synthesis in suppressing NO dependent inhibition of erythroid differentiation (Figure 5G).

We also tested the response of Irg1-/- mice to PHZ induced acute hemolytic anemia. Nrf2 protein levels increased in the spleen on days 3 and 5 during the recovery from PHZ-induced anemia (Figure 6A and S5B). These data are consistent with the in vivo metabolomics analysis on days 1 and 3 after PHZ treatment showed increased levels of itaconate in Kit+SEPs (Figure 6B). However, Irg1-/- has less Nrf2 protein in the spleen on day 3 when compared to control mice (Figure 6A). Analysis of Nrf2 target gene expression showed a delay at day 1 after

PHZ treatment (Figure 6C). The mRNA expression of erythroid genes was similarly delayed in Irg1-/- mice, however this decrease occurred only in the early time points and expression increased at later time points during recovery (Figure 6D). The increase in stress BFU-E was also delayed, which resulted in Irg1-/- mice reaching their lowest hematocrit levels a day earlier than control mice (Figure 6E). These defects were not caused by lower levels of Epo or a delay in increasing Epo levels in the serum (Fig S5C). Although the Irg1-/- mice exhibited defects, they were transient and the Irg1-/- mice eventually reached levels of erythroid gene expression, stress BFU-E and hematocrit similar to controls (Figure 6D-E). These data suggest that an alternative mechanism to activate Nrf2 compensates during the recovery from acute anemia.

Itaconate activates Nrf2-mediated SEP differentiation.

Culturing SEPs in SEEM maintains the transient amplifying population of erythroid progenitors. Switching the cultures to SEDM leads to commitment to erythroid differentiation and loss of self-renewal ability[16, 18]. This switch leads to an increase in erythroid gene expression and a loss of pro-inflammatory gene expression (Figure S4A). In contrast, Gene set enrichment analysis of our RNA-seq data of control and Nrf2-/- SEPs isolated on SEDM day 3 showed that Nrf2 mutant SEPs fail to upregulate erythroid genes[39]. Conversely, they maintain the expression of pro-inflammatory signals (Figure 7A-B). Furthermore, the Nrf2-/- SEPS fail to increase the expression of genes involved in ribosome biogenesis and amino acid metabolism, suggesting a decline of translational efficiency for hemoglobin production (Figure S6A). The RNA-seq data is consistent with the data showing that mutation of Nrf2 blocks the ability of exogenous OI to inhibit proliferation of SEPs cultured in SEEM (Figure 3D-F). These data suggest that the anti-inflammatory signals provided by itaconate promote SEP differentiation through Nrf2 activation. To demonstrate that activation of Nrf2 drives differentiation, we cultured SEPs from wildtype control and Irg1-/- in SEDM media. Compared to wildtype controls, Irg1-/- SEPs expressed significantly lower mRNA levels of representative erythroid genes, EpoR, Gata1 and Cpox. However, if the cultures were treated with OI or DMF, a known Nrf2 activator, we observed

significantly increased expression of EpoR, Gata1 and Cpox with OI while DMF significantly increased EpoR and showed a trend towards increased Gata1 and Cpox mRNA expression (Figure 7C). Analysis of BFU-E colony forming cells showed that mutation of Irg1 significantly decreased the frequency of BFU-E generated in the culture. Treatment with OI significantly increased the frequency BFU-E in Irg1-/- cultures and to lesser extent so did DMF (Figure 7D). These data show that increasing Nrf2 activity drives the differentiation of Seps that lack the ability to generate itaconate and underscore the ability of itaconate to promote differentiation.

Discussion

Protective immunity must balance the need to increase the production of myeloid effector cells with the need to maintain erythroid homeostasis. To accomplish these goals, pro-inflammatory cytokines that increase myelopoiesis also promote stress erythropoiesis to compensate for the loss of steady state erythroid output[13, 40]. Here we present data that further underscore how changes in inflammatory signals regulate stress erythropoiesis. TNFα and NO play key roles during the expansion stage, but the transition to differentiation is characterized by a loss of pro-inflammatory signals and increase in anti-inflammatory signals and a change in metabolism (Ruan et al. bioRxiv[25], unpublished data)[17, 41]. Our data show that increased production of itaconate in SEPs in part catalyzes this transition. One target of itaconate is Nrf2 and our data is consistent with Nrf2 and Irg1 acting in a cell autonomous manner. Nrf2 is well known as a regulator of oxidative stress[32, 42] and the increased Nrf2 activity coincides with decreases in NO as SEPs transition to differentiation. Decreasing NO production is a key target of this Itaconate-Nrf2 pathway. Our data showed that itaconate decreased Nos2 mRNA, but the protein levels and Nos2+ cells as identified by flow cytometry did not decline to similarly low levels. Despite the lack of a decrease in Nos2 protein, NO MFI did decrease in SEPs upon itaconate treatment. NO production can be regulated at multiple levels. Arginine can be used by Nos2 to make NO or used to generate polyamines through the action of arginase 1[43]. We observed that arginase 1 (Arg1) mRNA expression increases when SEPs are switched into differentiation media, which

supports the idea that arginine metabolism changes during the commitment to differentiation (data not shown).

Although we have focused on the role of itaconate in activating the Nrf2 pathway, other known itaconate targets could also play a role in stress erythropoiesis. Itaconate is known to inhibit Tet2 to dampen inflammatory responses in macrophages[44]. Recent work from Tseng et al. showed that Tet2 plays a role in SEP differentiation[45]. Further work will be needed to delineate the roles of itaconate and Tet2 during the transition to differentiation. Although we have focused on events in SEPs, itaconate is a well-known anti-inflammatory metabolite in macrophages and others have shown that mutation of Nrf2 decreases macrophage populations in erythroblastic islands in the bone marrow and spleen during recovery from phlebotomy[34]. These data suggest that these mediators could also affect the niche and the extent of that contribution is not known.

Marcero et al. showed that exogenous itaconate could inhibit heme biosynthesis in MEL cells[46]. Our analysis examined SEPs that are more immature than MEL cells, which correspond to post stress BFU-E, late stage SEPs[47]. These data suggest that itaconate production by SEPs and the niche must be decreased for terminal differentiation. Our previous work showed that peroxisome proliferator activated receptor γ (PPARγ) activation in niche macrophages plays a role in promoting the transition to differentiation[18]. Irg1 expression is regulated by PPARγ, so increased PPARγ activity at this time could decrease itaconate levels so as not to impeded heme biosynthesis[48]. This idea is consistent with our RNAseq data which showed that PPARγ expression increases more than 3-fold when SEPs commit to differentiation. Future work will be needed to address this question.

Irg1-/- mice exhibit defects in the recovery from HKBA and to a lesser extent from PHZ induced anemia. The mutant mice eventually recover from PHZ induced anemia and the expression of Nrf2 target genes during recovery is only delayed in Irg1-/- mice. These data

suggest that a signal other than itaconate increases Nrf2 activity. Our preliminary data suggests that IL-10 plays a role in maintaining Nrf2 activity during differentiation of SEPs. Its expression increases both in vitro and in vivo when SEPs commit to differentiation. Exogenous IL-10 increases stress BFU-E formation (Data not shown). IL-10 has not been previously implicated in stress erythropoiesis. In fact, transgenic over-expression of IL-10 increases myelopoiesis and causes anemia, which suggests that the levels, duration and site of IL-10 expression may affect the response in the erythroid lineage[49]. Similarly, other non-erythroid cytokines may play a role in stress erythropoiesis. IL-33 inhibits bone marrow erythropoiesis and can cause anemia, but it also induces the formation of iron recycling macrophages and increases the production itaconate and anti-inflammatory factors including IL-10[7, 50]. These data suggest that other pro-inflammatory or alarmin signals could play roles in stress erythropoiesis that are distinct from their effects on steady state erythropoiesis.

In summary, our data show that inflammatory signals that induce NO production are utilized by stress erythropoiesis to expand a population of immature progenitors, which is followed by a regulated resolution of inflammation to ensure a successful transition of early progenitors into mature erythrocytes to restore homeostasis.

Acknowledgments

We thank the members of the Paulson lab for suggestions on the work, especially Yuting Bai for her help with mice blood collection. We thank Sougat Misra for helpful discussion about metabolism. Our studies were greatly helped by Dr. Rajeswaran Mani and the Huck Institutes of the Life Sciences Flow cytometry Facility (RRID:SCR_024460), Dr. Ashley Shay, Philip Smith and Justin Munro and the Huck Institutes of the Life Sciences Metabolomics facility

(RRIS:SCR_023864). This work was supported by NIH grant HL146528 and DK138865 (RFP), USDA-NIFA Hatch Project PEN04960 accession #7006577 (RFP) and USDA-NIFA Hatch Project PEN04932, accession #7006585 (KSP), R01CA239256 (MH), NIFA-USDA Hatch Project PEN04275 accession #1018544 (MH), startup funds from the College of Agricultural Sciences, Pennsylvania State University (MH), the Dr. Frances Keesler Graham Early Career Professorship from the Social Science Research Institute, Pennsylvania State University (MH), the USDA-NIFA Hatch Project PEN04917 accession number 7006412 (ADP) and from the PA Department of Health using Tobacco CURE funds (ADP, IK). SGT was supported by T32DK120509, AS was supported by T32GM108563.

Authorship

B.R., K.S.P and R.F.P. conceived and designed the study. B.R., S.T., M.C., AS, H.G. and Y.C. performed the experiments. B.R., J.M., and M.A.H. analyzed the RNA-seq data. B.R., I.K., J.C., and A.D.P. analyzed the metabolomics analysis. B.R. and R.F.P. wrote the initial draft of the manuscript, and all authors were involved in review and editing.

Conflict-of-interest disclosure: The authors declare no competing financial interests.

Figure legends

Figure 1. Itaconate levels increase during the transition to differentiation. (A) SEPs were isolated from SEEM cultures at day 1 and 3 for metabolomics analysis. Volcano plot showing the changes in metabolites between day 1 and 3 SEPs in SEEM (n=5 per time point). (B) Levels of itaconate relative to spike in chlorpropamide were calculated and normalized to SEEM day 5 (EM D5 = 1), N=5 per time point. (C) (Top) Expression of Irg1 mRNA (left) and protein (right) in Kit+ SEPs. (Bottom) Expression of Irg1 mRNA (left) and protein (right) stromal cells. Relative Irg1 mRNA expression was normalized to 18S rRNA. Irg1 Protein was normalized to β-actin levels using Image J software. N=3 per time point. Corresponding western blots are shown in Figure S1A. Data represent mean ± SEM. * $p < 0.05$, ** $p < 0.01$, *** $p < 0.001$.

Figure 2. Itaconate inhibits NO dependent proliferation of SEPs. (A) SEPs were treated ± 125 μM OI at indicated days of SEEM cultures. On day 5 of SEEM cultures, total SEP cell counts were measured (n=4 per group, one-way ANOVA/Dunnett's). (B) SEPs were treated ± 125 μM OI at SEEM day 3 for 48 hrs followed by flow cytometry analysis of SEPs. Representative flow cytometry plot showing pre-gated $Kit^{+}Sca1^{+}$cells with additional markers CD34 and CD133. (C) Quantification of percentages (left) and absolute number (right) of the indicated populations shown in panel B. (N=4 per group, unpaired t test). (D-F) SEPs were treated ± 125 μM OI at SEEM day 3 for 48 hrs. (D) Quantification of intracellular NO levels in $Kit^{+}Sca1^{+}$ SEPs by mean fluorescence intensity (MFI) of DAF-FM DA staining (left). Analysis of NO MFI in the indicated SEP populations (right) (n=3 per group, unpaired t test). (E) qRT-PCR analysis of Nos2 mRNA expression in SEPs on day 5 of SEEM culture treated ± with OI (N=4, unpaired t test). (F). Nos2 expression in stromal cells. SEP cultures were treated with OI as indicated above. On days 4 and 5 of SEEM culture stromal cells were analyzed by flow cytometry for Nos2 expression and markers for monocytes and macrophages as indicated. N=3 per time point, paired t-test). (G) SEEM cultures were treated with 125 μM OI alone or in

combination with SNAP at the indicated concentrations for 24 hrs. Flow cytometry quantification of numbers of Kit+Sca1+ SEPs (n=3 per group, one-way ANOVA/Tukey's). (H) WT and Irg1-/- SEPs were cultured in SEEM for 5 days. (Left) qRT-PCR analysis Nos2 mRNA expression and (right) flow cytometry quantification of absolute numbers of indicated populations of SEPs (n=4 per genotype, unpaired t test). Data represent mean ± SEM. * $p < 0.05$, ** $p < 0.01$, *** $p < 0.001$.

Figure 3. Itaconate impairs SEP proliferation in a Nrf2-dependent manner. (A) Nrf2 protein analysis in Kit+ SEPs (left) and stromal cells (right). Protein levels relative to Hsp70 were calculated using Image J (n=3 per time point Unpaired t-Test). Corresponding western blots are shown in Figure S2E. (B) Analysis of total SEP counts in WT and Nrf2-/- SEEM cultures at day 3 and 5 (n=5 per group, unpaired t test). (C) Flow cytometry quantification of the percentages (top) and absolute numbers (bottom) of indicated populations of SEPs in WT and Nrf2-/- SEEM cultures at day 5 (n=4 per group, unpaired t test). (D-F) WT and Nrf2-/- SEEM cultures were treated ± 125 μM OI for 3 days. qRT-PCR analysis of *Nqo1* expression (D), analysis for numbers of Kit+Sca1+ SEPs (E), and qRT-PCR analysis of *Nos2* expression. (n=4 (D-F), two-way ANOVA/Fisher's LSD).

Figure 4. Increased itaconate production during differentiation alleviates NO dependent erythroid inhibition. (A) SEPs were harvested from WT, or Irg1-/- cultures at SEEM Day 5 and SEDM Day 3. Western blot analysis of Nos2 protein expression, β-actin is a loading control. (B) (left) Analysis of Nos2 protein expression in wildtype control, Irg1-/- and Irg1-/- + 125 uM OI on day 3 of SEDM culture. β-actin is the loading control. (right) Nos2 protein levels calculated relative to β-actin calculated using Image J. (n=4, unpaired t-test). (C). Flow cytometry analysis of NO MFI from wildtype control, Irg1-/- and Irg1-/- + 125uM OI, analyzed on day 3 of SEDM

culture. (n=4, unpaired t-test). (D-F). SEPs isolated from wildtype SEDM cultures at day 3 were compared to Irg1-/- SEDM cultures treated ± 1400w for 3 days. (D). stress BFU-e, (E). Percent Kit+Sca1- SEPs at SEDM day 3, (F). mRNA expression of select erythroid genes, erythropoietin receptor (EpoR), coproporphyrinogen oxidase (Cpox), β-major globin (Hbb-b1) (N=4 per group, one way ANOVA/Tukey's)

Figure 5. Defective SEP differentiation in Irg1-deficient mice delayed the recovery from HKBA-induced inflammatory anemia. (A-G) Age- and sex-matched WT and Irg1-/- mice were administered with HKBA (5 x 10^8 particles/mouse) via intraperitoneal injection. (A) In the following 28 days, mice were monitored daily for survival and health, and blood was collected retro-orbitally in every other day for measurement of hematocrit (n=12 in WT, n=8 in Irg1-/-, repeated measures two-way ANOVA followed by unpaired t test). (B-C) Analysis of Hb (left) and RBC counts (right) concentrations (B), and measurement of spleen weight (left) and splenocyte numbers (right) (C) at indicated time points post HKBA injection (n=4 per group, unpaired t test). (D) Representative flow cytometry plot showing the gating of SEPs in the spleen isolated at day 8 post HKBA injection. (E-G) Analysis of percentages of Kit+Sca1-CD34-CD133- SEPs (E), frequency (top) and total numbers (bottom) of stress BFU-E colony formation (F), and *Nos2* mRNA abundance (G) at indicated time points (n=4 per group, unpaired t test).
Data represent mean ± SEM. * $p < 0.05$, ** $p < 0.01$, *** $p < 0.001$.

Figure 6. Irg1-/- mice exhibit a defect in recovery from phenylhydrazine induced acute hemolytic anemia. Wildtype mice were injected with phenylhydrazine (100 mg/Kg mouse) and analyzed on the indicated days. (A). Nrf2 protein expression in the spleen on the indicated days was determined by western blot analysis. β-actin is shown as a loading control. Corresponding western blots are shown in Figure S5B. (B). Metabolomic analysis of Itaconate levels in Kit+

SEPs isolated fromthe spleen on day 0, 1 and 3 after PHZ treatment. (n=5 per day). (C). qRT-PCR analysis of mRNA expression of Nrf2 target genes, Nqo1 and glutamate-cysteine ligase, modifier subunit (Gclm), in the spleen of wildtype and Irg1-/- mice on the indicated days of recovery from PHZ induced anemia. (n=3 per time point, unpaired t-test). (D) qRT-PCR analysis of select erythroid genes in the spleen of wildtype and Irg1-/- mice on the indicated days of recovery from PHZ induced anemia. (n=3 per time point, unpaired t-test). (E). Number of stress BFU-E in the spleen (left) and hematocrit (right) on the indicated days in wildtype and Irg1-/- mice treated with PHZ. (n=3 per time point, unpaired t-test).

Figure 7. Activation of Nrf2 promotes differentiation. (A-B). Gene set enrichment analysis[39] of control and Nrf2-/- SEDM day 3 RNA-seq data. (A) Analysis of gene sets involved in erythrocyte development, homeostasis and heme biosynthesis and (B) Inflammatory pathways. (C-D). SEPs were harvested from WT, or Irg1-/- SEDM cultures treated with vehicle, 125 μM OI or 30 μM DMF for 3 days. Analysis of mRNA expression of erythroid-specific genes by qRT-PCR (C). Analysis of stress BFU-E by colony assay (D) (n=4 per group, one-way ANOVA/Tukey's).

References

1. Palis J. Primitive and definitive erythropoiesis in mammals. Front Physiol. 2014;5:3. Epub 2014/01/31. doi: 10.3389/fphys.2014.00003. PubMed PMID: 24478716; PMCID: PMC3904103.

2. Klei TR, Meinderts SM, van den Berg TK, van Bruggen R. From the Cradle to the Grave: The Role of Macrophages in Erythropoiesis and Erythrophagocytosis. Front Immunol. 2017;8:73. Epub 2017/02/18. doi: 10.3389/fimmu.2017.00073. PubMed PMID: 28210260; PMCID: PMC5288342.

3. Buck I, Morceau F, Cristofanon S, Heintz C, Chateauvieux S, Reuter S, Dicato M, Diederich M. Tumor necrosis factor alpha inhibits erythroid differentiation in human erythropoietin-dependent cells involving p38 MAPK pathway, GATA-1 and FOG-1

downregulation and GATA-2 upregulation. Biochem Pharmacol. 2008;76(10):1229-39. Epub 2008/09/23. doi: 10.1016/j.bcp.2008.08.025. PubMed PMID: 18805401.

4. Dulmovits BM, Tang Y, Papoin J, He M, Li J, Yang H, Addorisio ME, Kennedy L, Khan M, Brindley E, Ashley RJ, Ackert-Bicknell C, Hale J, Kurita R, Nakamura Y, Diamond B, Barnes BJ, Hermine O, Gallagher PG, Steiner LA, Lipton JM, Taylor N, Mohandas N, Andersson U, Al-Abed Y, Tracey KJ, Blanc L. HMGB1-mediated restriction of EPO signaling contributes to anemia of inflammation. Blood. 2022;139(21):3181-93. Epub 2022/01/19. doi: 10.1182/blood.2021012048. PubMed PMID: 35040907; PMCID: PMC9136881.

5. Pietras EM, Mirantes-Barbeito C, Fong S, Loeffler D, Kovtonyuk LV, Zhang S, Lakshminarasimhan R, Chin CP, Techner JM, Will B, Nerlov C, Steidl U, Manz MG, Schroeder T, Passegué E. Chronic interleukin-1 exposure drives haematopoietic stem cells towards precocious myeloid differentiation at the expense of self-renewal. Nat Cell Biol. 2016;18(6):607-18. Epub 2016/04/26. doi: 10.1038/ncb3346. PubMed PMID: 27111842; PMCID: PMC4884136.

6. Subotički T, Ajtić OM, Đikić D, Santibanez JF, Tošić M, Čokić VP. Nitric Oxide Synthase Dependency in Hydroxyurea Inhibition of Erythroid Progenitor Growth. Genes (Basel). 2021;12(8). Epub 2021/08/28. doi: 10.3390/genes12081145. PubMed PMID: 34440315; PMCID: PMC8391407.

7. Swann JW, Koneva LA, Regan-Komito D, Sansom SN, Powrie F, Griseri T. IL-33 promotes anemia during chronic inflammation by inhibiting differentiation of erythroid progenitors. J Exp Med. 2020;217(9). Epub 2020/06/11. doi: 10.1084/jem.20200164. PubMed PMID: 32520308; PMCID: PMC7478740

8. Zamai L, Secchiero P, Pierpaoli S, Bassini A, Papa S, Alnemri ES, Guidotti L, Vitale M, Zauli G. TNF-related apoptosis-inducing ligand (TRAIL) as a negative regulator of normal human erythropoiesis. Blood. 2000;95(12):3716-24. Epub 2000/06/14. PubMed PMID: 10845902.

9. Bian Z, Shi L, Guo YL, Lv Z, Tang C, Niu S, Tremblay A, Venkataramani M, Culpepper C, Li L, Zhou Z, Mansour A, Zhang Y, Gewirtz A, Kidder K, Zen K, Liu Y. Cd47-Sirpα interaction and IL-10 constrain inflammation-induced macrophage phagocytosis of healthy self-cells. Proc Natl Acad Sci U S A. 2016;113(37):E5434-43. Epub 2016/09/01. doi: 10.1073/pnas.1521069113. PubMed PMID: 27578867; PMCID: PMC5027463.

10. Libregts SF, Gutiérrez L, de Bruin AM, Wensveen FM, Papadopoulos P, van Ijcken W, Ozgür Z, Philipsen S, Nolte MA. Chronic IFN-γ production in mice induces anemia by reducing erythrocyte life span and inhibiting erythropoiesis through an IRF-1/PU.1 axis. Blood. 2011;118(9):2578-88. Epub 2011/07/05. doi: 10.1182/blood-2010-10-315218. PubMed PMID: 21725055.

11. Liu W, Östberg N, Yalcinkaya M, Dou H, Endo-Umeda K, Tang Y, Hou X, Xiao T, Fidler TP, Abramowicz S, Yang YG, Soehnlein O, Tall AR, Wang N. Erythroid lineage Jak2V617F expression promotes atherosclerosis through erythrophagocytosis and macrophage ferroptosis. J Clin Invest. 2022;132(13). Epub 2022/05/20. doi: 10.1172/jci155724. PubMed PMID: 35587375; PMCID: PMC9246386.

12. Wang W, Liu W, Fidler T, Wang Y, Tang Y, Woods B, Welch C, Cai B, Silvestre-Roig C, Ai D, Yang YG, Hidalgo A, Soehnlein O, Tabas I, Levine RL, Tall AR, Wang N. Macrophage Inflammation, Erythrophagocytosis, and Accelerated Atherosclerosis in Jak2 (V617F) Mice. Circ Res. 2018;123(11):e35-e47. Epub 2018/12/21. doi: 10.1161/circresaha.118.313283. PubMed PMID: 30571460; PMCID: PMC6309796.

13. Paulson RF, Ruan B, Hao S, Chen Y. Stress Erythropoiesis is a Key Inflammatory Response. Cells. 2020;9(3). Epub 2020/03/12. doi: 10.3390/cells9030634. PubMed PMID: 32155728; PMCID: PMC7140438.

14. Harandi OF, Hedge S, Wu DC, McKeone D, Paulson RF. Murine erythroid short-term radioprotection requires a BMP4-dependent, self-renewing population of stress erythroid progenitors. J Clin Invest. 2010;120(12):4507-19. Epub 2010/11/10. doi: 10.1172/JCI41291. PubMed PMID: 21060151; PMCID: 2993581.

15. Liao C, Prabhu KS, Paulson RF. Monocyte-derived macrophages expand the murine stress erythropoietic niche during the recovery from anemia. Blood. 2018;132(24):2580-93. Epub 2018/10/17. doi: 10.1182/blood-2018-06-856831. PubMed PMID: 30322871; PMCID: PMC6293871

16. Xiang J, Wu DC, Chen Y, Paulson RF. In vitro culture of stress erythroid progenitors identifies distinct progenitor populations and analogous human progenitors. Blood. 2015;125(11):1803-12. Epub 2015/01/23. doi: 10.1182/blood-2014-07-591453. PubMed PMID: 25608563; PMCID: 4357585.

17. Bennett LF, Liao C, Quickel MD, Yeoh BS, Vijay-Kumar M, Hankey-Giblin P, Prabhu KS, Paulson RF. Inflammation induces stress erythropoiesis through heme-dependent activation of SPI-C. Sci Signal. 2019;12(598). Epub 2019/09/12. doi: 10.1126/scisignal.aap7336. PubMed PMID: 31506384.

18. Chen Y, Xiang J, Qian F, Diwakar BT, Ruan B, Hao S, Prabhu KS, Paulson RF. Epo receptor signaling in macrophages alters the splenic niche to promote erythroid differentiation. Blood. 2020;136(2):235-46. Epub 2020/05/01. doi: 10.1182/blood.2019003480. PubMed PMID: 32350523; PMCID: PMC7357191

19. Hao S, Xiang J, Wu DC, Fraser JW, Ruan B, Cai J, Patterson AD, Lai ZC, Paulson RF. Gdf15 regulates murine stress erythroid progenitor proliferation and the development of the stress erythropoiesis niche. Blood Adv. 2019;3(14):2205-17. Epub 2019/07/22. doi: 10.1182/bloodadvances.2019000375. PubMed PMID: 31324641; PMCID: PMC6650738

20. Lenox LE, Perry JM, Paulson RF. BMP4 and Madh5 regulate the erythroid response to acute anemia. Blood. 2005;105(7):2741-8. Epub 2004/12/14. doi: 10.1182/blood-2004-02-0703. PubMed PMID: 15591122.

21. Perry JM, Harandi OF, Paulson RF. BMP4, SCF, and hypoxia cooperatively regulate the expansion of murine stress erythroid progenitors. Blood. 2007;109(10):4494-502. Epub 2007/02/08. doi: 10.1182/blood-2006-04-016154. PubMed PMID: 17284534; PMCID: PMC1885504.

22. Perry JM, Harandi OF, Porayette P, Hegde S, Kannan AK, Paulson RF. Maintenance of the BMP4-dependent stress erythropoiesis pathway in the murine spleen requires hedgehog signaling. Blood. 2009;113(4):911-8. Epub 2008/10/18. doi: 10.1182/blood-2008-03-147892. PubMed PMID: 18927434; PMCID: PMC2630276.

23. Mantovani A, Sica A, Sozzani S, Allavena P, Vecchi A, Locati M. The chemokine system in diverse forms of macrophage activation and polarization. Trends Immunol. 2004;25(12):677-86. Epub 2004/11/09. doi: 10.1016/j.it.2004.09.015. PubMed PMID: 15530839.

24. O'Neill LAJ, Artyomov MN. Itaconate: the poster child of metabolic reprogramming in macrophage function. Nat Rev Immunol. 2019;19(5):273-81. Epub 2019/02/02. doi: 10.1038/s41577-019-0128-5. PubMed PMID: 30705422.

25. Ruan B, Chen Y, Trimidal S, Koo I, Qian F, Cai J, McGuigan J, Hall MA, Patterson AD, Prabhu KS, Paulson RF. Nitric oxide regulates metabolism in murine stress erythroid progenitors to promote recovery during inflammatory anemia. bioRxiv. 2023. Epub 2023/03/23. doi: 10.1101/2023.03.11.532207. PubMed PMID: 36945370; PMCID: PMC10028999.

26. Chan K, Lu R, Chang JC, Kan YW. NRF2, a member of the NFE2 family of transcription factors, is not essential for murine erythropoiesis, growth, and development. Proc Natl Acad Sci U S A. 1996;93(24):13943-8. Epub 1996/11/26. doi: 10.1073/pnas.93.24.13943. PubMed PMID: 8943040; PMCID: PMC19474.

27. Kühn R, Löhler J, Rennick D, Rajewsky K, Müller W. Interleukin-10-deficient mice develop chronic enterocolitis. Cell. 1993;75(2):263-74. Epub 1993/10/22. doi: 10.1016/0092-8674(93)80068-p. PubMed PMID: 8402911.

28. Bennett LF, Liao C, Paulson RF. Stress Erythropoiesis Model Systems. Methods Mol Biol. 2018;1698:91-102. Epub 2017/10/28. doi: 10.1007/978-1-4939-7428-3_5. PubMed PMID: 29076085; PMCID: PMC6510234.

29. Gardenghi S, Renaud TM, Meloni A, Casu C, Crielaard BJ, Bystrom LM, Greenberg-Kushnir N, Sasu BJ, Cooke KS, Rivella S. Distinct roles for hepcidin and interleukin-6 in the recovery from anemia in mice injected with heat-killed Brucella

abortus. Blood. 2014;123(8):1137-45. Epub 2013/12/21. doi: 10.1182/blood-2013-08-521625. PubMed PMID: 24357729; PMCID: PMC3931188.

30. Michelucci A, Cordes T, Ghelfi J, Pailot A, Reiling N, Goldmann O, Binz T, Wegner A, Tallam A, Rausell A, Buttini M, Linster CL, Medina E, Balling R, Hiller K. Immune-responsive gene 1 protein links metabolism to immunity by catalyzing itaconic acid production. Proc Natl Acad Sci U S A. 2013;110(19):7820-5. Epub 2013/04/24. doi: 10.1073/pnas.1218599110. PubMed PMID: 23610393; PMCID: PMC3651434.

31. Hooftman A, O'Neill LAJ. The Immunomodulatory Potential of the Metabolite Itaconate. Trends Immunol. 2019;40(8):687-98. Epub 2019/06/11. doi: 10.1016/j.it.2019.05.007. PubMed PMID: 31178405.

32. Mills EL, Ryan DG, Prag HA, Dikovskaya D, Menon D, Zaslona Z, Jedrychowski MP, Costa ASH, Higgins M, Hams E, Szpyt J, Runtsch MC, King MS, McGouran JF, Fischer R, Kessler BM, McGettrick AF, Hughes MM, Carroll RG, Booty LM, Knatko EV, Meakin PJ, Ashford MLJ, Modis LK, Brunori G, Sévin DC, Fallon PG, Caldwell ST, Kunji ERS, Chouchani ET, Frezza C, Dinkova-Kostova AT, Hartley RC, Murphy MP, O'Neill LA. Itaconate is an anti-inflammatory metabolite that activates Nrf2 via alkylation of KEAP1. Nature. 2018;556(7699):113-7. Epub 2018/03/29. doi: 10.1038/nature25986. PubMed PMID: 29590092; PMCID: PMC6047741.

33. Singh RJ, Hogg N, Joseph J, Kalyanaraman B. Mechanism of nitric oxide release from S-nitrosothiols. J Biol Chem. 1996;271(31):18596-603. Epub 1996/08/02. doi: 10.1074/jbc.271.31.18596. PubMed PMID: 8702510.

34. Gbotosho OT, Kapetanaki MG, Ross M, Ghosh S, Weidert F, Bullock GC, Watkins S, Ofori-Acquah SF, Kato GJ. Nrf2 deficiency in mice attenuates erythropoietic stress-related macrophage hypercellularity. Exp Hematol. 2020;84:19-28.e4. Epub 2020/03/11. doi: 10.1016/j.exphem.2020.02.005. PubMed PMID: 32151553; PMCID: PMC7237317.

35. Nguyen T, Huang HC, Pickett CB. Transcriptional regulation of the antioxidant response element. Activation by Nrf2 and repression by MafK. J Biol Chem. 2000;275(20):15466-73. Epub 2000/04/05. doi: 10.1074/jbc.M000361200. PubMed PMID: 10747902.

36. Garvey EP, Oplinger JA, Furfine ES, Kiff RJ, Laszlo F, Whittle BJ, Knowles RG. 1400W is a slow, tight binding, and highly selective inhibitor of inducible nitric-oxide synthase in vitro and in vivo. J Biol Chem. 1997;272(8):4959-63. Epub 1997/02/21. doi: 10.1074/jbc.272.8.4959. PubMed PMID: 9030556.

37. Kim A, Fung E, Parikh SG, Valore EV, Gabayan V, Nemeth E, Ganz T. A mouse model of anemia of inflammation: complex pathogenesis with partial dependence on hepcidin. Blood. 2014;123(8):1129-36. Epub 2013/12/21. doi: 10.1182/blood-2013-08-521419. PubMed PMID: 24357728; PMCID: PMC9632791.

38. Millot S, Andrieu V, Letteron P, Lyoumi S, Hurtado-Nedelec M, Karim Z, Thibaudeau O, Bennada S, Charrier JL, Lasocki S, Beaumont C. Erythropoietin stimulates spleen BMP4-dependent stress erythropoiesis and partially corrects anemia in a mouse model of generalized inflammation. Blood. 2010;116(26):6072-81. Epub 2010/09/17. doi: 10.1182/blood-2010-04-281840. PubMed PMID: 20844235.

39. Subramanian A, Tamayo P, Mootha VK, Mukherjee S, Ebert BL, Gillette MA, Paulovich A, Pomeroy SL, Golub TR, Lander ES, Mesirov JP. Gene set enrichment analysis: a knowledge-based approach for interpreting genome-wide expression profiles. Proc Natl Acad Sci U S A. 2005;102(43):15545-50. Epub 2005/10/04. doi: 10.1073/pnas.0506580102. PubMed PMID: 16199517; PMCID: PMC1239896.

40. Paulson RF, Hariharan S, Little JA. Stress erythropoiesis: definitions and models for its study. Exp Hematol. 2020;89:43-54.e2. Epub 2020/08/05. doi: 10.1016/j.exphem.2020.07.011. PubMed PMID: 32750404; PMCID: PMC7508762.

41. Ruan B, Paulson RF. Metabolic regulation of stress erythropoiesis, outstanding questions, and possible paradigms. Front Physiol. 2022;13:1063294. Epub 2023/01/24. doi: 10.3389/fphys.2022.1063294. PubMed PMID: 36685181; PMCID: PMC9849390.

42. Yang L, Chen Y, He S, Yu D. The crucial role of NRF2 in erythropoiesis and anemia: Mechanisms and therapeutic opportunities. Arch Biochem Biophys. 2024;754:109948. Epub 2024/03/08. doi: 10.1016/j.abb.2024.109948. PubMed PMID: 38452967.

43. Caldwell RW, Rodriguez PC, Toque HA, Narayanan SP, Caldwell RB. Arginase: A Multifaceted Enzyme Important in Health and Disease. Physiol Rev. 2018;98(2):641-65. Epub 2018/02/08. doi: 10.1152/physrev.00037.2016. PubMed PMID: 29412048; PMCID: PMC5966718.

44. Chen LL, Morcelle C, Cheng ZL, Chen X, Xu Y, Gao Y, Song J, Li Z, Smith MD, Shi M, Zhu Y, Zhou N, Cheng M, He C, Liu KY, Lu G, Zhang L, Zhang C, Zhang J, Sun Y, Qi T, Lyu Y, Ren ZZ, Tan XM, Yin J, Lan F, Liu Y, Yang H, Qian M, Duan C, Chang X, Zhou Y, Shen L, Baldwin AS, Guan KL, Xiong Y, Ye D. Itaconate inhibits TET DNA dioxygenases to dampen inflammatory responses. Nat Cell Biol. 2022;24(3):353-63. Epub 2022/03/09. doi: 10.1038/s41556-022-00853-8. PubMed PMID: 35256775; PMCID: PMC9305987.

45. Tseng YJ, Kageyama Y, Murdaugh RL, Kitano A, Kim JH, Hoegenauer KA, Tiessen J, Smith MH, Uryu H, Takahashi K, Martin JF, Samee MAH, Nakada D. Increased iron uptake by splenic hematopoietic stem cells promotes TET2-dependent erythroid regeneration. Nat Commun. 2024;15(1):538. Epub 2024/01/16. doi: 10.1038/s41467-024-44718-0. PubMed PMID: 38225226; PMCID: PMC10789814.

46. Marcero JR, Cox JE, Bergonia HA, Medlock AE, Phillips JD, Dailey HA. The immunometabolite itaconate inhibits heme synthesis and remodels cellular metabolism in erythroid precursors. Blood Adv. 2021;5(23):4831-41. Epub 2021/09/08. doi: 10.1182/bloodadvances.2021004750. PubMed PMID: 34492704; PMCID: PMC9153040.

47. Hegde S, Hankey P, Paulson RF. Self-renewal of leukemia stem cells in Friend virus-induced erythroleukemia requires proviral insertional activation of Spi1 and hedgehog signaling but not mutation of p53. Stem Cells. 2012;30(2):121-30. Epub 2011/11/16. doi: 10.1002/stem.781. PubMed PMID: 22083997; PMCID: PMC3341850.

48. Nelson VL, Nguyen HCB, Garcìa-Cañaveras JC, Briggs ER, Ho WY, DiSpirito JR, Marinis JM, Hill DA, Lazar MA. PPARγ is a nexus controlling alternative activation of macrophages via glutamine metabolism. Genes Dev. 2018;32(15-16):1035-44. Epub 2018/07/15. doi: 10.1101/gad.312355.118. PubMed PMID: 30006480; PMCID: PMC6075146.

49. Cardoso A, Martins AC, Maceiras AR, Liu W, Castro I, Castro AG, Bandeira A, Di Santo JP, Cumano A, Li Y, Vieira P, Saraiva M. Interleukin-10 induces interferon-γ-dependent emergency myelopoiesis. Cell Rep. 2021;37(4):109887. Epub 2021/10/28. doi: 10.1016/j.celrep.2021.109887. PubMed PMID: 34706233.

50. Lu Y, Basatemur G, Scott IC, Chiarugi D, Clement M, Harrison J, Jugdaohsingh R, Yu X, Newland SA, Jolin HE, Li X, Chen X, Szymanska M, Haraldsen G, Palmer G, Fallon PG, Cohen ES, McKenzie ANJ, Mallat Z. Interleukin-33 Signaling Controls the Development of Iron-Recycling Macrophages. Immunity. 2020;52(5):782-93.e5. Epub 2020/04/10. doi: 10.1016/j.immuni.2020.03.006. PubMed PMID: 32272082; PMCID: PMC7237885.

Figure 1

A

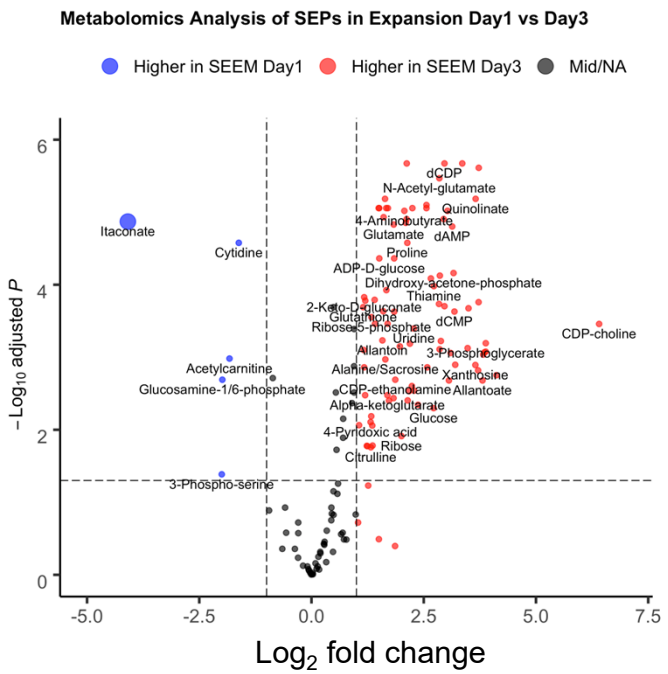

B

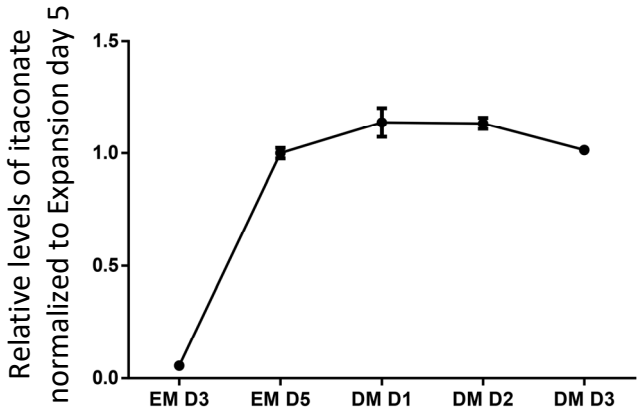

C

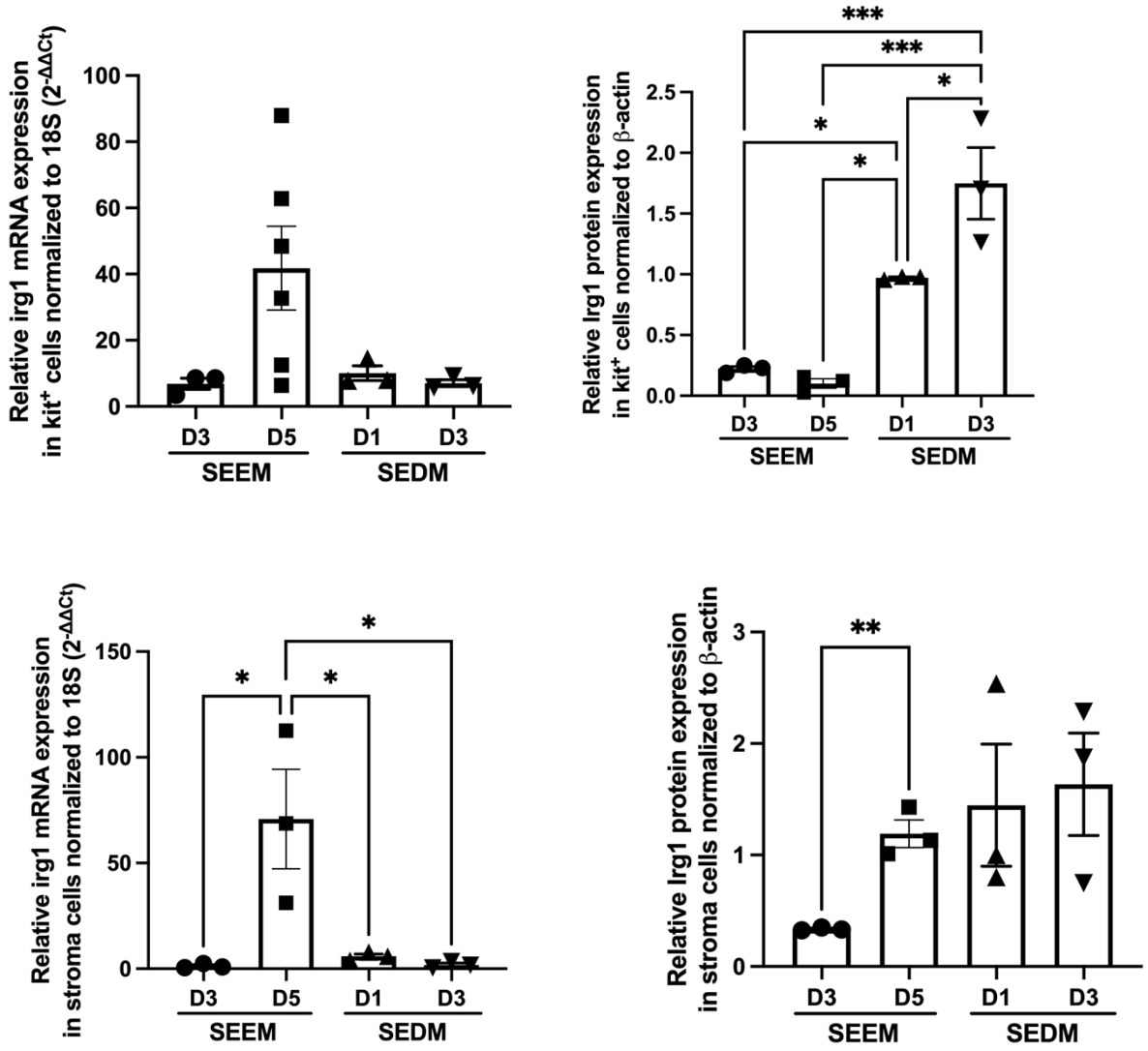

Figure 1.

Figure 2

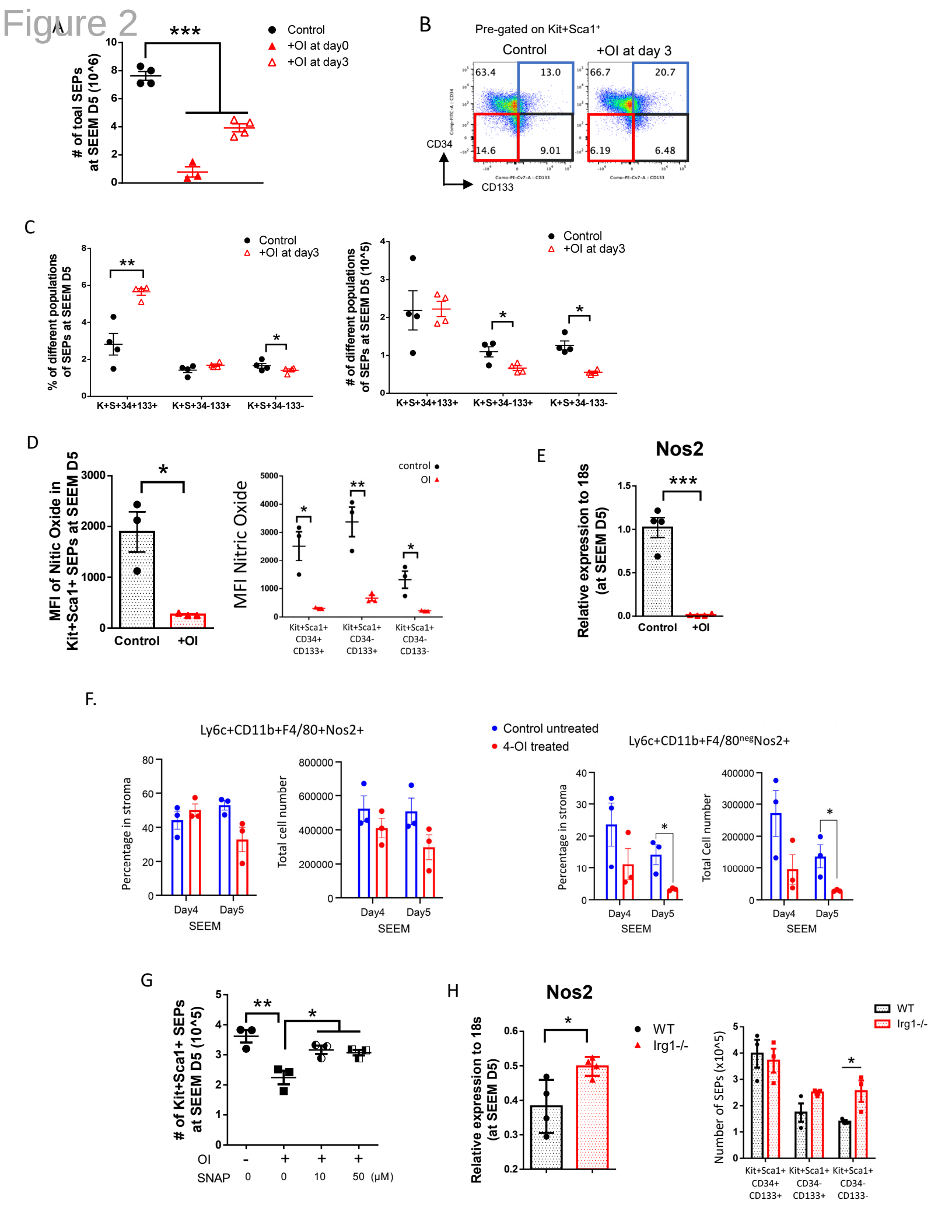
A
***
Control
+OI at day0
+OI at day3
# of toal SEPs at SEEM D5 (10^6)
B
Pre-gated on Kit+Sca1+
Control
+OI at day 3
63.4
13.0
14.6
9.01
66.7
20.7
6.19
6.48
CD34
CD133
C
Control
+OI at day3
% of different populations of SEPs at SEEM D5
# of different populations of SEPs at SEEM D5 (10^5)
K+S+34+133+
K+S+34-133+
K+S+34-133-
D
MFI of Nitic Oxide in Kit+Sca1+ SEPs at SEEM D5
Control
+OI
MFI Nitric Oxide
control
OI
Kit+Sca1+ CD34+ CD133+
Kit+Sca1+ CD34- CD133+
Kit+Sca1+ CD34- CD133-
E
Nos2
Relative expression to 18s (at SEEM D5)
Control
+OI
F.
Ly6c+CD11b+F4/80+Nos2+
Control untreated
4-OI treated
Ly6c+CD11b+F4/80negNos2+
Percentage in stroma
Total cell number
Day4
Day5
SEEM
G
# of Kit+Sca1+ SEPs at SEEM D5 (10^5)
OI
SNAP
0
0
10
50 (μM)
H
Nos2
Relative expression to 18s (at SEEM D5)
WT
Irg1-/-
Number of SEPs (x10^5)
Kit+Sca1+ CD34+ CD133+
Kit+Sca1+ CD34- CD133+
Kit+Sca1+ CD34- CD133-

Figure 3

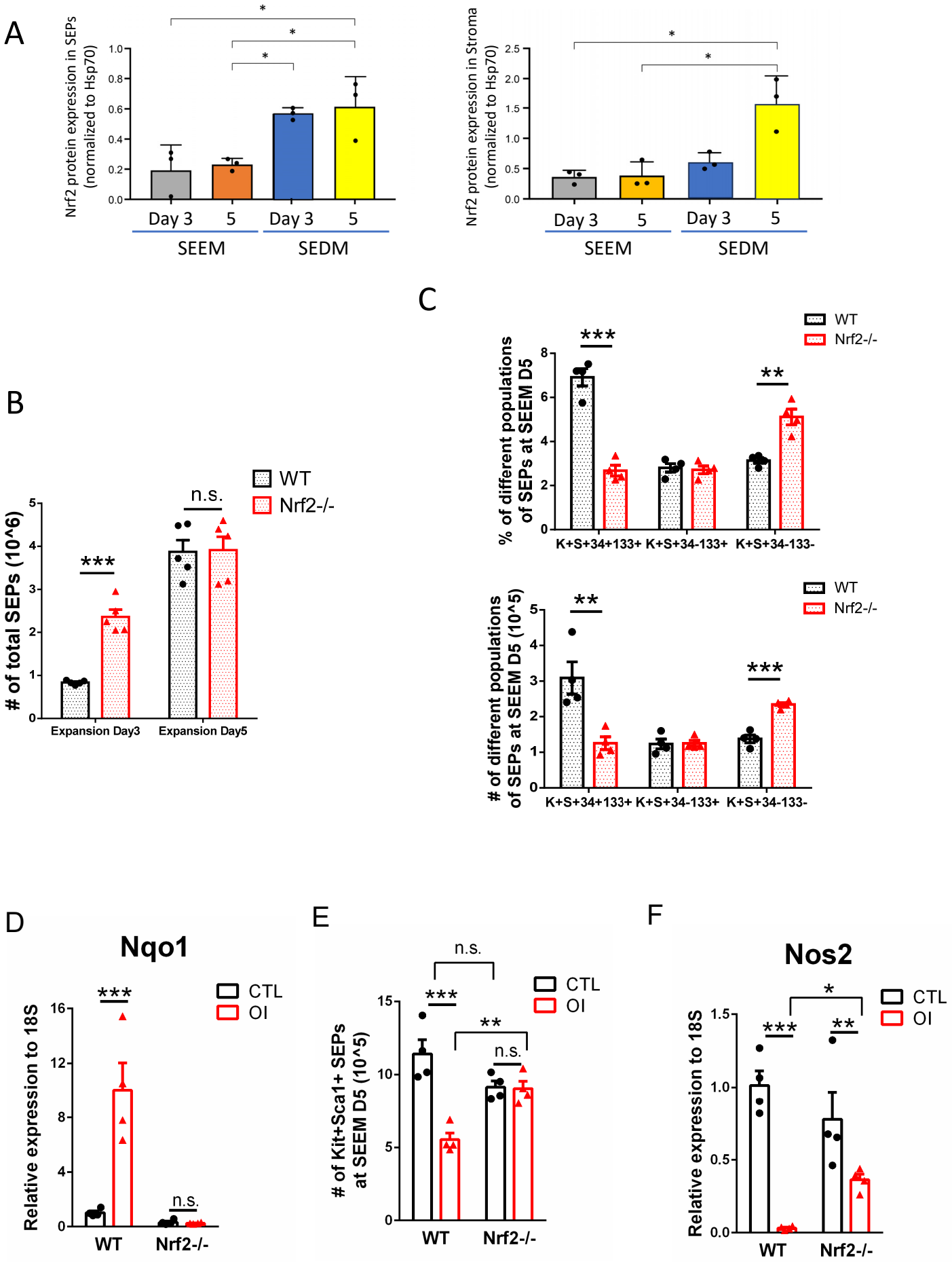
A
Nrf2 protein expression in SEPs (normalized to Hsp70)
Day 3
5
Day 3
5
SEEM
SEDM
Nrf2 protein expression in Stroma (normalized to Hsp70)
B
# of total SEPs (10^6)
WT
Nrf2-/-
n.s.
Expansion Day3
Expansion Day5
C
% of different populations of SEPs at SEEM D5
K+S+34+133+
K+S+34-133+
K+S+34-133-
# of different populations of SEPs at SEEM D5 (10^5)
D
Nqo1
Relative expression to 18S
CTL
OI
WT
Nrf2-/-
E
# of Kit+Sca1+ SEPs at SEEM D5 (10^5)
F
Nos2

Figure 4

Figure 4

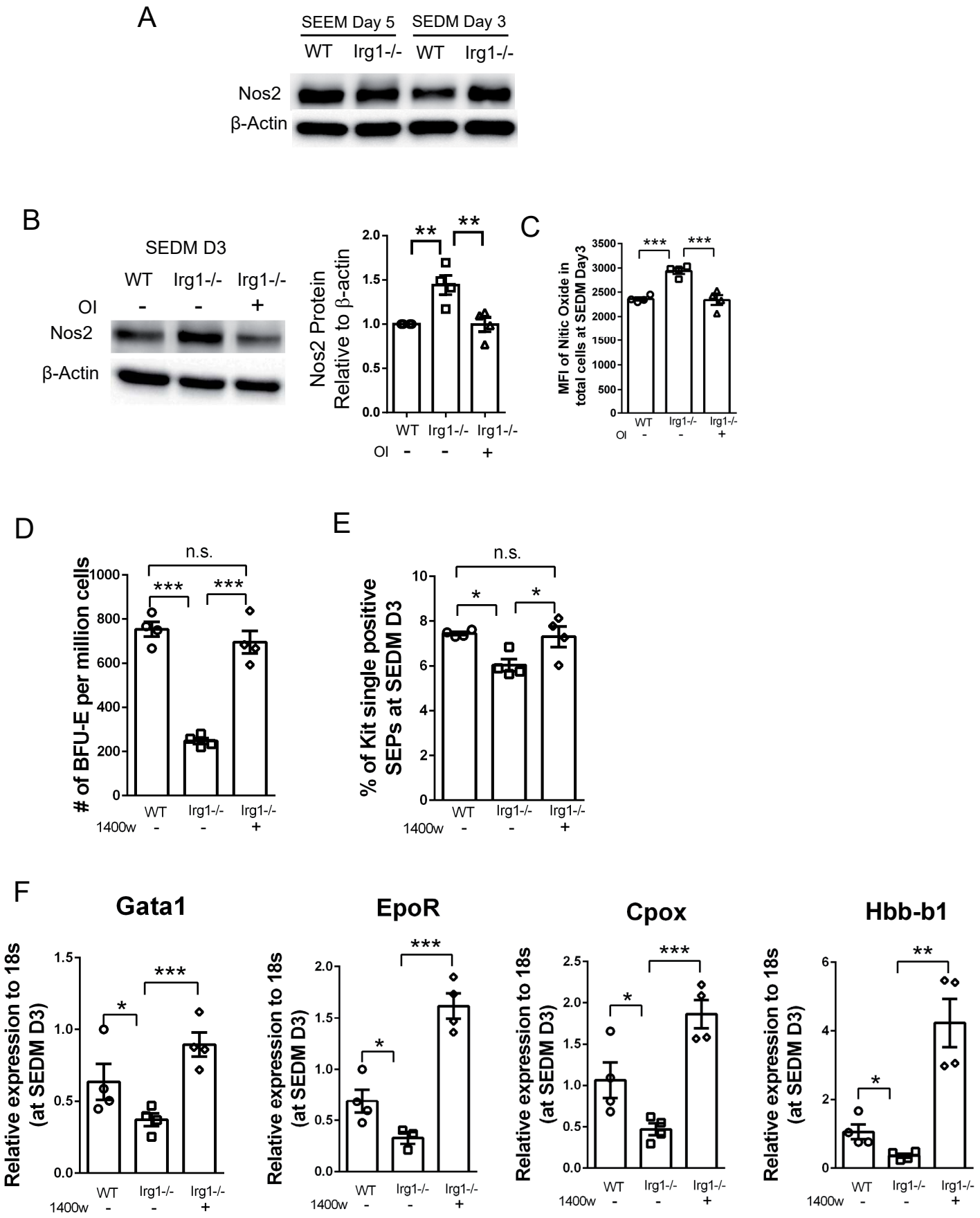

Figure 5

A

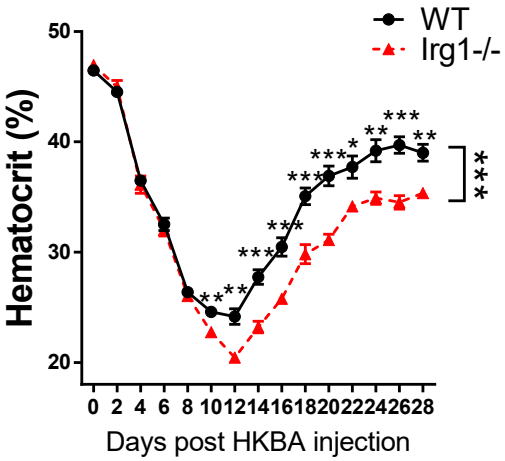

B

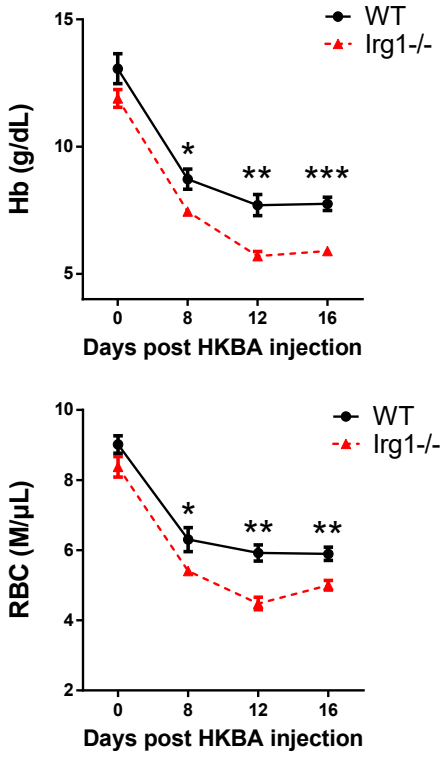

C

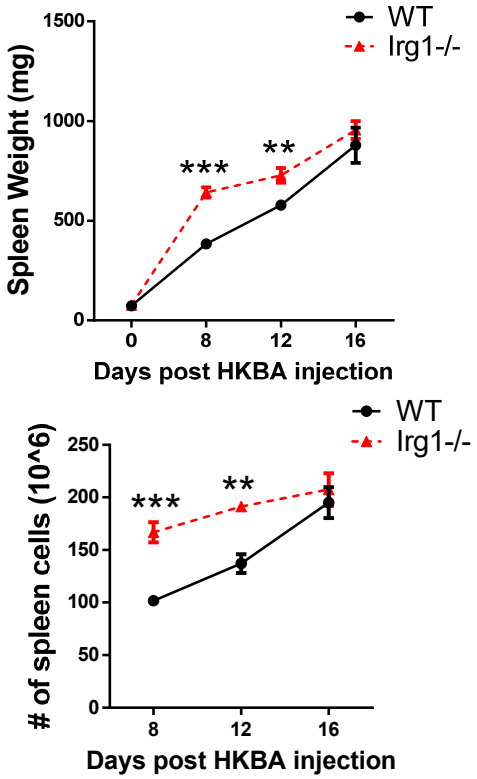

D

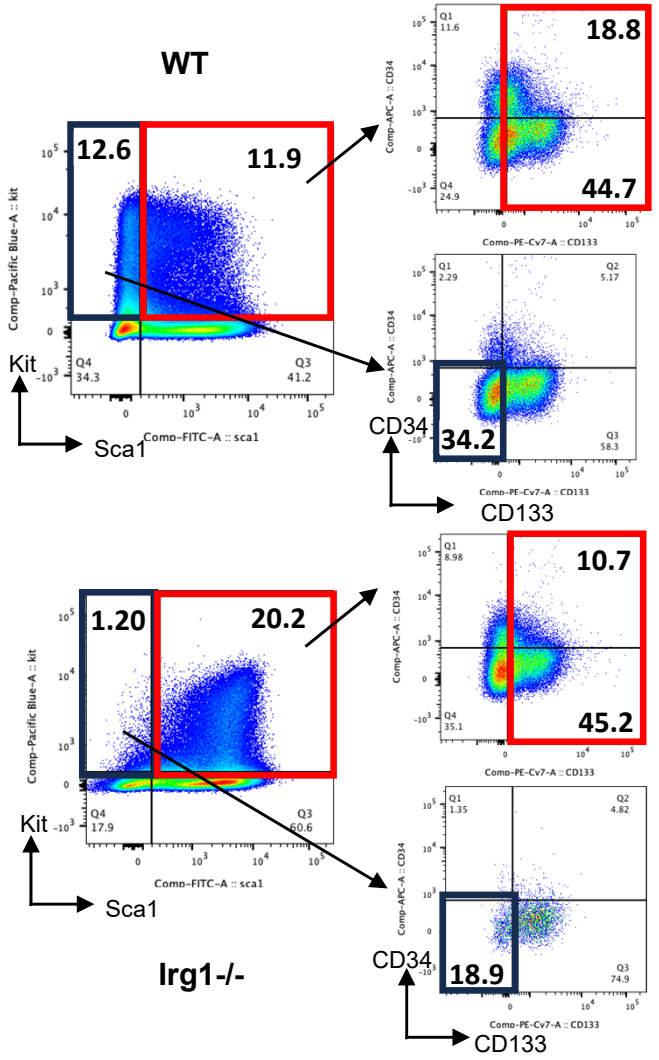

E

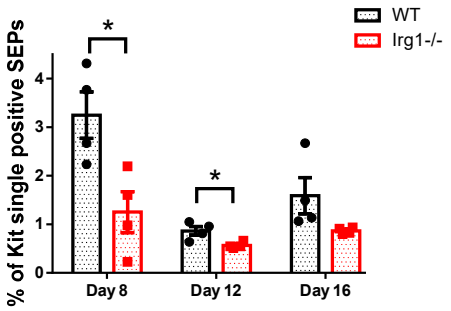

F

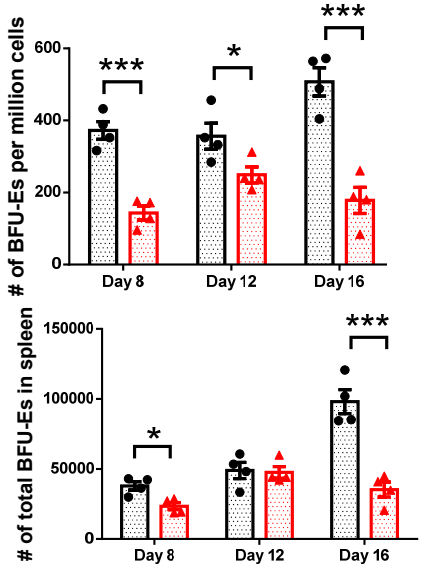

G

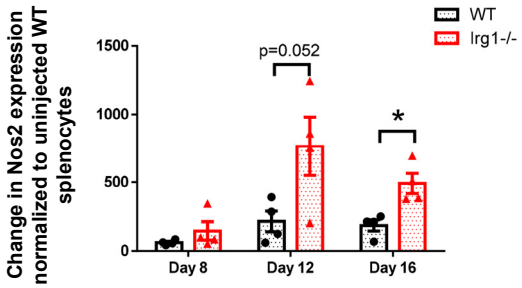

Figure 6

A.

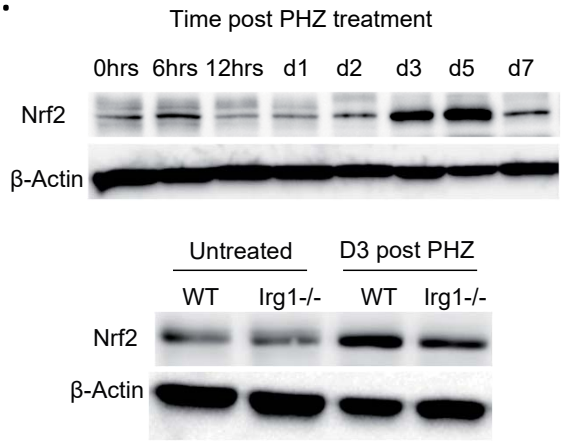

B.

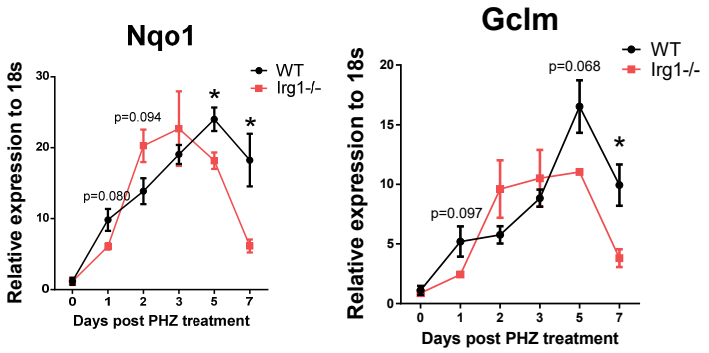

C.

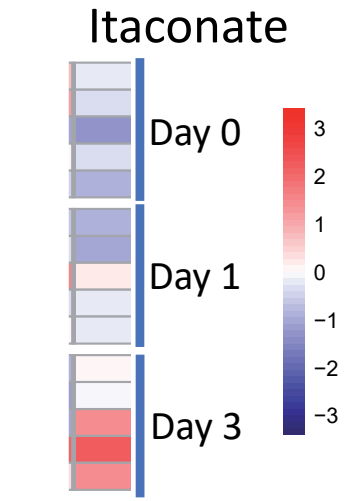

D.

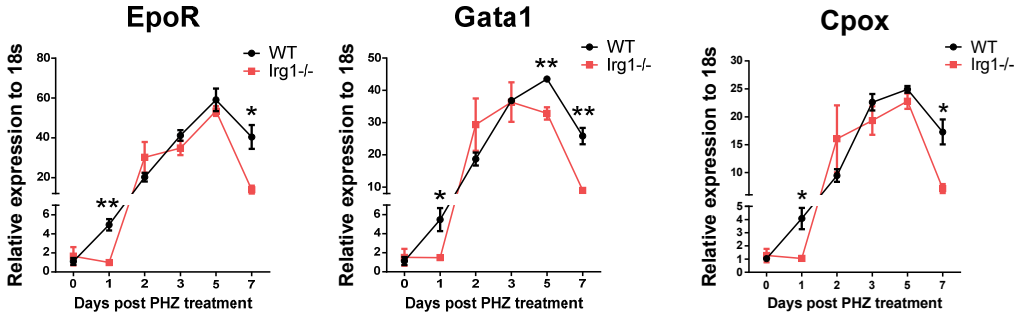

E

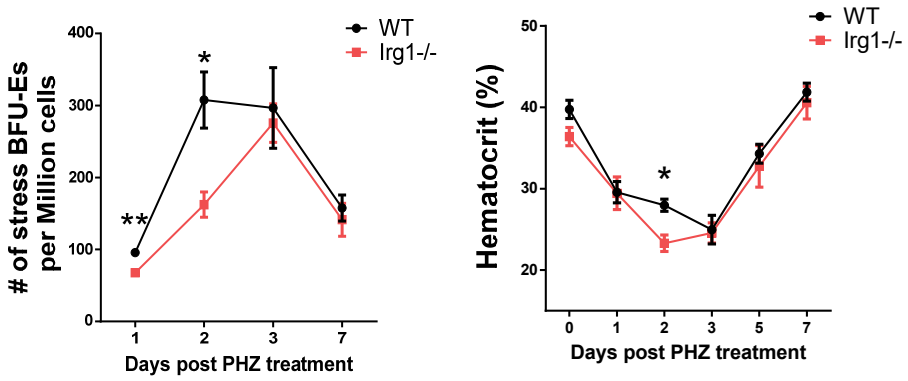

Figure 7

A.

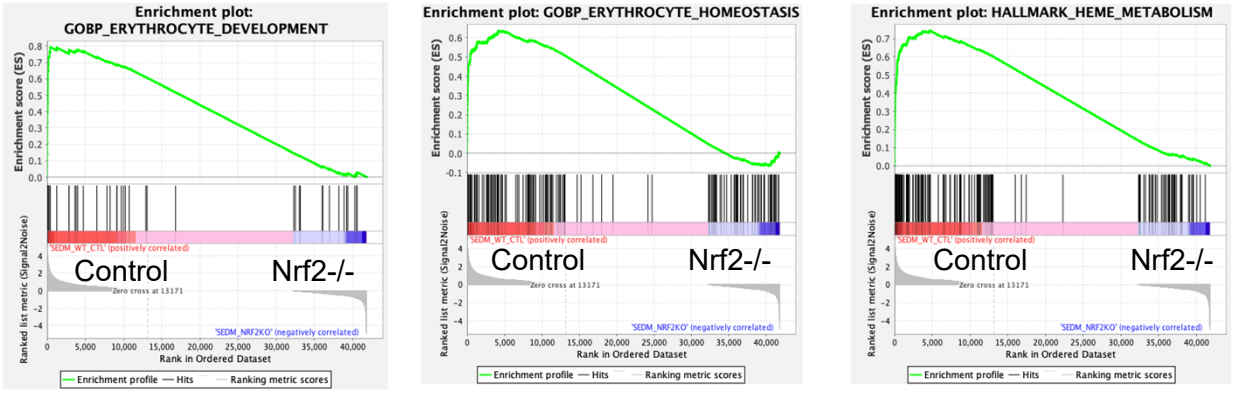

B.

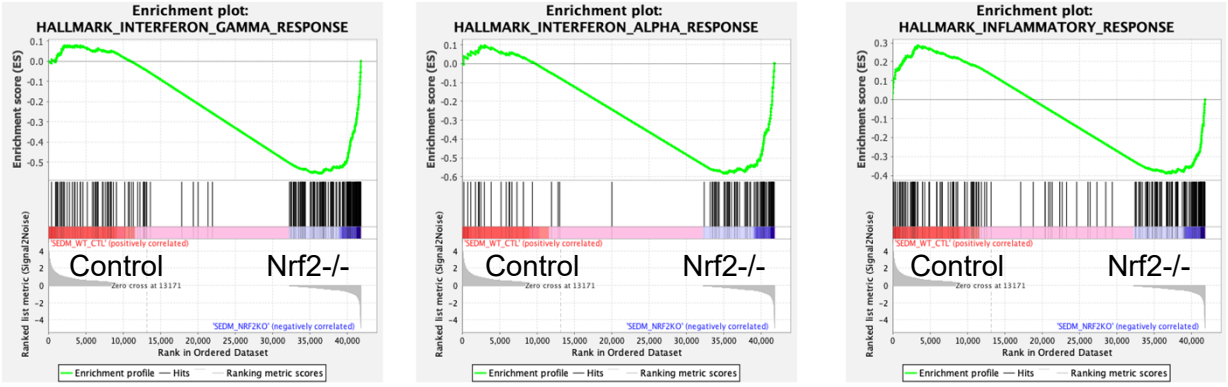

C.

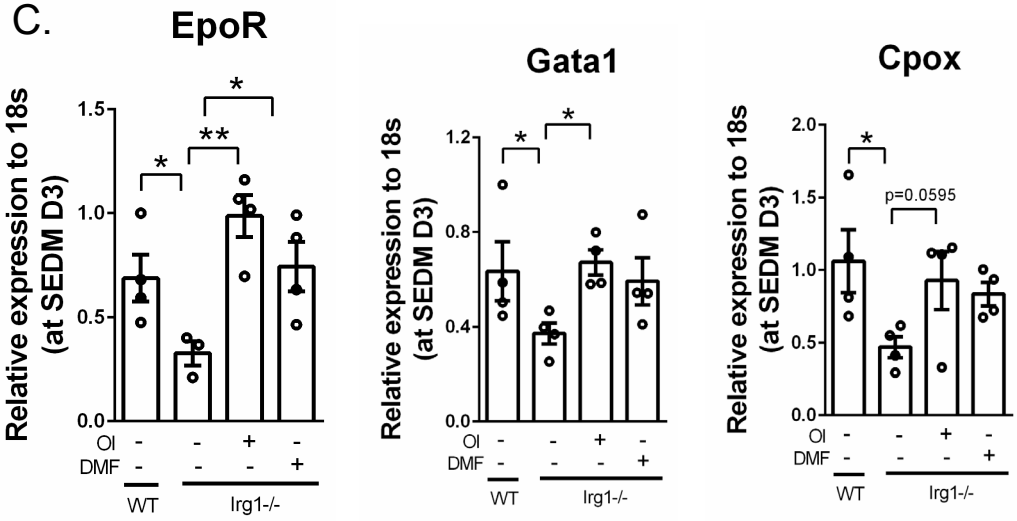

D.

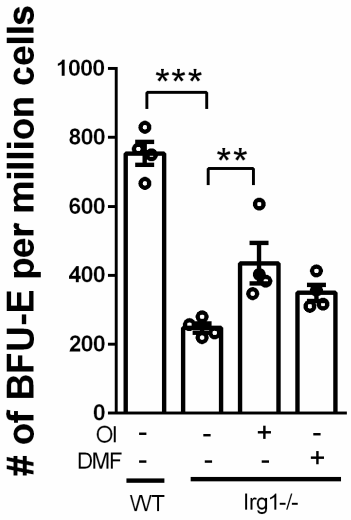

Supplemental Methods

Stress erythropoiesis expansion and differentiation medium[1]

Stress erythropoiesis expansion medium (SEEM) was prepared by supplementing IMDM with 10% (v/v) FBS, 0.0007% (v/v) 2-mercaptoethanol, 0.01 g/ml BSA, 10 µg/ml ciprofloxacin, 2 mM L-glutamine, 10 µg/ml insulin, 200 µg/ml holo-transferrin, 50 ng/ml murine SCF, 15 ng/ml human BMP4, 25 ng/ml murine SHH and 30 ng/ml murine GDF15. Stress erythropoiesis differentiation medium (SEDM) was prepared by additionally supplementing SEEM with 3 U/ml human Epo. SEEM were cultured in ambient air (20% O_2), while SEDM were cultured in a hypoxia chamber (2% O_2) to maximize differentiation potential. All cultures were incubated in 5% CO_2 at 37 °C.

Stress erythropoiesis cultures

Bone marrow cells were isolated, and cells were plated into stress erythropoiesis expansion media (SEEM) at a starting concentration of 6 x 10^5 cells/ml for a 5-day culture. For differentiation cultures, non-adherent cells harvested from SEEM cultures were resuspended in stress erythropoiesis differentiation media (SEDM) at 3 x 10^5 cells/ml for another 3 days.

In vivo induction of stress erythropoiesis

Phenylhydrazine was used to induce stress erythropoiesis in the context of acute hemolytic anemia. Mice were injected intraperitoneally with a single dose (100 mg/kg body weight) of freshly prepared phenylhydrazine (Sigma-Aldrich, dissolved in PBS)[2]. Blood and spleen samples were collected at indicated time points post injection for downstream analysis.

Heat-killed Brucella abortus (HKBA, strain 1119-3) was used to induce anemia of inflammation according to a previously described method[3]. After centrifuging, HKBA was resuspended in PBS to make a stock solution with a concentration of 5 x 10^9 particles/ml. HKBA stock was 1:1 diluted with PBS before use. To induce stress erythropoiesis, age- and sex-matched mice were administered with 200 µl diluted HKBA (5 x 10^8 particles/mouse) via intraperitoneal injection. In the following 28 days, mice were monitored daily for survival and health, and blood was collected retro-orbitally in every other day for microhematocrit test. To

27 assess stress erythropoiesis, mice were sacrificed at indicated time points for blood and spleen
28 collection.

29 **Hematocrit measurement and complete blood count test**

30 To determine hematocrit levels by microhematocrit method, the peripheral blood was collected
31 retro-orbitally with the heparin-coated microhematocrit tube (VWR). The tube with one end
32 sealed (CRITOSEAL, Leica Microsystems) was centrifuged for 5 min at 11,700 rpm (Autocrit
33 Ultra 3 microhematocrit centrifuge, BD Biosciences) to separate the blood sample. The
34 hematocrit level was quantified as the percentage of the volume of packed red blood cells
35 relative to the volume of whole blood. For complete blood count analysis, mouse blood was
36 collected retro-orbitally with a K_2EDTA-coated Microtainer tube, and sample was immediately
37 analyzed on a Hemavet 950 analyzer (Drew Scientific).

38 **Stress BFU-E colony assay[(2)]**

39 SEPs isolated from SEDM cultures or mouse splenocytes were counted using a
40 hemocytometer. For each sample, 2.5 x 10^5 cells were resuspended in 2 ml MethoCult M3334
41 media (STEMCELL Technologies) supplemented additionally with 50 ng/ml SCF (GoldBio) and
42 15 ng/ml BMP4 (Thermo Fisher Scientific), and cell suspension was evenly plated into 3 wells of
43 a 12-well plate as technical triplicates. Stress BFU-E colonies were stained with benzidine and
44 quantified after a 5-day culture in 37 °C with 2% O_2 and 5% CO_2.

45 **Flow cytometry analysis**

46 Cells were stained with Zombie Yellow Fixable Viability Kit (BioLegend) to exclude dead cells.
47 After 15 min incubation at room temperature in the dark, cells were washed and prepared in
48 single cell suspension in flow cytometry staining buffer. The combinations of fluorophore-
49 conjugated cell surface antibodies were added to the cell suspension. For analysis of mouse
50 stress erythroid progenitors, the following antibodies were used: Kit Brilliant Violet 421 (Clone
51 2B8, BioLegend), Sca-1 APC/Cyanine7 (Clone D7, BioLegend), Sca-1 FITC (Clone D7,
52 BioLegend), CD34 Alexa Fluor 647 (Clone RAM34, BD Biosciences), CD34 FITC (Clone

53 RAM34, BD Biosciences), and CD133 PE/Cyanine7 (Clone 315-2C11, BioLegend). For CD45.1
54 WT/CD45.2 Nrf2-/-co-culture experiment, the above antibodies were added together with
55 CD45.2 FITC (Clone 104, BD Biosciences) to determine the cell sources. After 30 min
56 incubation on ice in the dark, cells were washed twice and resuspended in 250 µl staining
57 buffer. Flow cytometry analysis was performed on a BD LSR Fortessa Cytometer (BD
58 Biosciences) and data were analyzed by FlowJo software (BD Biosciences). Intracellular NO
59 was analyzed by flow cytometry using the fluorescent probe DAF-FM diacetate according to
60 vendor's instruction (Thermo Fisher Scientific). See Table S2 for a list of antibodies used.

61 **qRT-PCR**

62 Total RNA was extracted with TRIzol reagent (Thermo Fisher Scientific). 1 µg of total RNA was
63 reverse transcribed to cDNA using the qScript cDNA Synthesis Kit (Quanta Biosciences).
64 TaqMan Gene Expression assays were performed on a StepOnePlus Real-Time PCR System
65 (Applied Biosystems) using the PerfeCTa qPCR SuperMix ROX (Quanta Biosciences). Relative
66 gene expression was quantified by the $\Delta\Delta C_T$ method in reference to the housekeeping gene
67 18S rRNA for normalization. See Table S3 for TaqMan probes.

68 **Western blot**

69 Spleen cells or cultured progenitor cells were lysed with RIPA Buffer (Thermo Fisher Scientific)
70 in combination with protease inhibitor cocktail (Sigma-Aldrich) and PMSF (Cell Signaling
71 Technology). Cultured cell lysates were vortexed and spleen cell lysates were briefly sonicated
72 using a Bioruptor Standard Sonicator. Samples were incubated on ice for 30 min and
73 centrifuged at 13,000 g for 15 min at 4°C. Protein concentration was quantified using the Pierce
74 BCA Protein Assay Kit (Thermo Fisher Scientific) following manufacturer's protocol. 30 µg of
75 total proteins were subjected to SDS-PAGE and transferred onto a PVDF membrane. The
76 membranes were blocked with 5% milk in TBST at room temperature for 1 hrs and
77 immunoblotted with primary antibodies against Nrf2 (1:1000, Proteintech), iNOS (1:1000,
78 Cayman Chemical), Irg-1 (Cell Signaling Technology), Hsp70 (abcam 1:2000) and β-Actin

79 (1:2000, Santa Cruz) overnight at 4°C. The blots were washed with TBST for three times,
80 followed by incubation with HRP-conjugated secondary antibodies (1:5000, Thermo Fisher
81 Scientific) for 1 hrs at room temperature. The blots were developed using SuperSignal West
82 Pico PLUS Chemiluminescent Substrate (Thermo Fisher Scientific) and imaged on a G:BOX
83 Chemi XX6 gel imager (Syngene). Image J software (National Institutes of Health) was used for
84 densitometry band quantification.

85 **Gene Set Enrichment Analysis (GSEA)**

86 Gene Set Enrichment Analysis (GSEA) was performed using the GSEA software (GSEA_4.3.2)
87 available at https://www.gsea-msigdb.org/gsea/index.jsp, a joint project of UC San Diego and
88 the Broad Institute. The analysis was conducted using the Molecular Signatures Database
89 (MSigDB) gene sets. Differentially expressed genes from the dataset were ranked based on
90 their signal-to-noise ratio, and enrichment was evaluated against the predefined gene sets to
91 identify pathways and processes associated with the experimental conditions. Results were
92 considered significant at a false discovery rate (FDR) < 0.25, as recommended by the GSEA
93 guidelines. The GSEA software and methodology were used as described in Subramanian,
94 Tamayo, et al. and Mootha, Lindgren, et al.[4, 5].

95 **Supplementary table 1. Gene set enrichment analysis**

96 Figure S4

	GOBP Erythrocyte development	GOBP Erythrocyte homeostasis	Hallmark Heme metabolism
Gene set size	48	160	188
Nominal enrichment score (NES)	1.889	1.443	1.750
FDR q-value	0.15	0.840	0.0003
Nominal p score	0.0	0.005	0.0

97

	GOBP Positive regulation of cytokine production involved in immune response	GOBP Positive regulation of innate immune response
Gene set size	84	140

Nominal enrichment score (NES)	-1.565	-1.503
FDR q-value	0.249	0.344
Nominal p score	0.003	0.002

	GOBP Response to interferon alpha	GOBP Response to interferon beta
Gene set size	31	65
Nominal enrichment score (NES)	-1.543	-1.90
FDR q-value	0.284	0.001
Nominal p score	0.009	0.0

Figure S6

	WP_Amino_Acid_Metabolism	GOCC_Ribosome
Gene set size	95	236
Nominal enrichment score (NES)	1.636	1.333
FDR q-value	0.066	0.484
Nominal p score	0.0	0.003

Figure 7

	GOBP Erythrocyte development	GOBP Erythrocyte homeostasis	Hallmark Heme metabolism
Gene set size	48	160	188
Nominal enrichment score (NES)	1.753	1.58	1.867
FDR q-value	0.10	0.169	0.0
Nominal p score	0.0	0.0	0.0

	Hallmark interferon gamma response	Hallmark interferon alpha response	Hallmark Inflammatory response
Gene set size	188	94	197
Nominal enrichment score (NES)	-1.753	-1.698	-1.234
FDR q-value	0.0	0.001	0.126
Nominal p score	0.0	0.0	0.0

106 **Supplemental Table 2. Flow cytometry antibody list**

Antibodies	Source	Identifier
Brilliant Violet 421 anti-mouse CD117 (c-Kit), Clone 2B8	BioLegend	Cat# 105828; RRID: AB_11204256
APC/Cyanine7 anti-mouse Ly-6A/E (Sca-1), Clone D7	BioLegend	Cat# 108126; RRID: AB_10645327
FITC anti-mouse Ly-6A/E (Sca-1), Clone D7	BioLegend	Cat# 108106; RRID: AB_313343
PE/Cyanine7 anti-mouse CD133, Clone 315-2C11	BioLegend	Cat# 141210; RRID: AB_2564069
Alexa Fluor 647 anti-mouse CD34, Clone RAM34	BD Biosciences	Cat# 560230; RRID: AB_1645200
FITC anti-mouse CD34, Clone RAM34	BD Biosciences	Cat# 553733; RRID: AB_395017
FITC anti-mouse CD45.2, Clone 104	BD Biosciences	Cat# 553772; RRID: AB_395041
Brilliant Violet 421 anti-human CD117 (c-kit), Clone 104D2	BioLegend	Cat# 313216; RRID: AB_11148721
APC anti-mouse/human CD11B clone M1/70	BioLegend	Catelog#101212; RRID AB_312795
Alexa-Fluor 647 anti-mouse CD106 (Vcam1), clone 429	BioLegend	Catalog #105711; RRID AB_493430
Brilliant violet 421 anti-mouse Ly-6C, Clone HK1.4	BioLegend	Catalog #128031; RRID: AB_256177
PE/Cy7 anti-mouse F4/80, clone BM8	Biolegend	catalog # 123114; RRID: AB_893490

107

108

109 **Supplemental Table 3. List of TaqMan probes for qRT-PCR.**

Probes and primers	Identifier
Mouse Nos2	Mm00440502_m1
Mouse Irg1	Mm01224532_m1
Mouse Nfe2l2	Mm00477784_m1
Mouse Nqo1	Mm01253561_m1
Mouse Gata1	Mm01352636_m1
Mouse EpoR	Mm00833882_m1
Mouse Cpox	Mm00483982_m1
Mouse Gclm	Mm01324400_m1
Mouse Gsr	Mm00439154_m1
Mouse Tnf	Mm00443258_m1
Mouse Hif1a	Mm00458869_m1
Mouse Pdk1	Mm00554300_m1
Mouse SLC48A1 (Hrg1)	Mm00728070_s1
Mouse β Major Probe	6FAM- CTCTCTTGGGAACAATTAACCATTGTTCACAG-TAMRA
Mouse β Major Forward Primer	5’ -AACCCCCTTTCCTGCTCTTG- 3’
Mouse β Major Reverse Primer	5’ -TCATTTTGCCAACAACTGACAGA- 3’
Mouse β H1 Probe	6FAM- ACTTTCTTGCCATGGGCTCTAATCCGG-TAMRA
Mouse β H1 Forward Primer	5’ -CCTGGCCATCATGGGAAAC- 3’
Mouse β H1 Reverse Primer	5’-CCCCAAGCCCAAGGATGT-3’

110

111

112

Supplementary 1

A

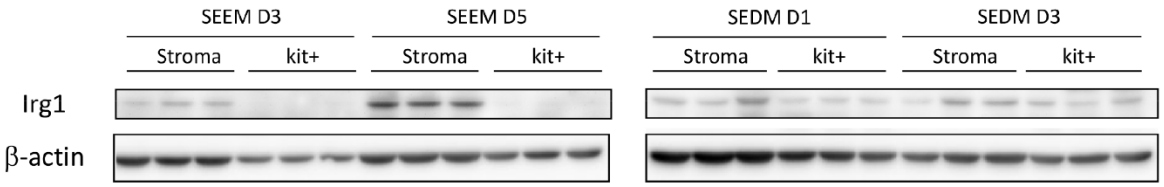

B

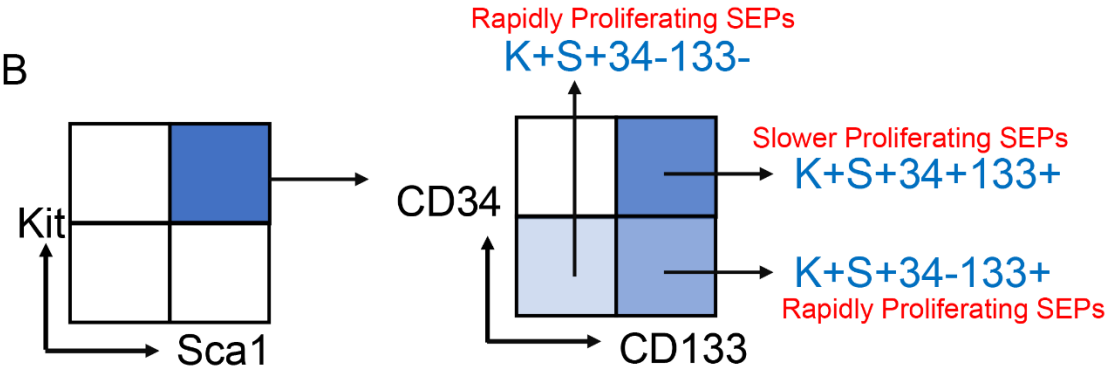

C

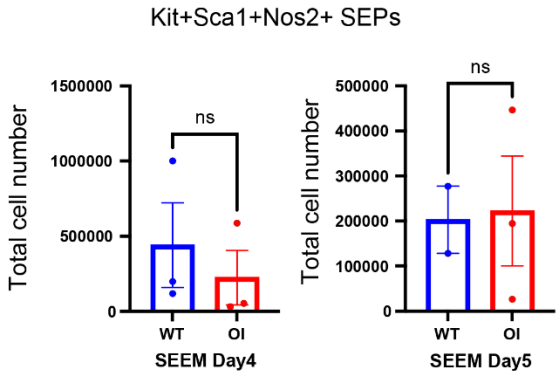

113

114
115

C.

SEEM Day 5

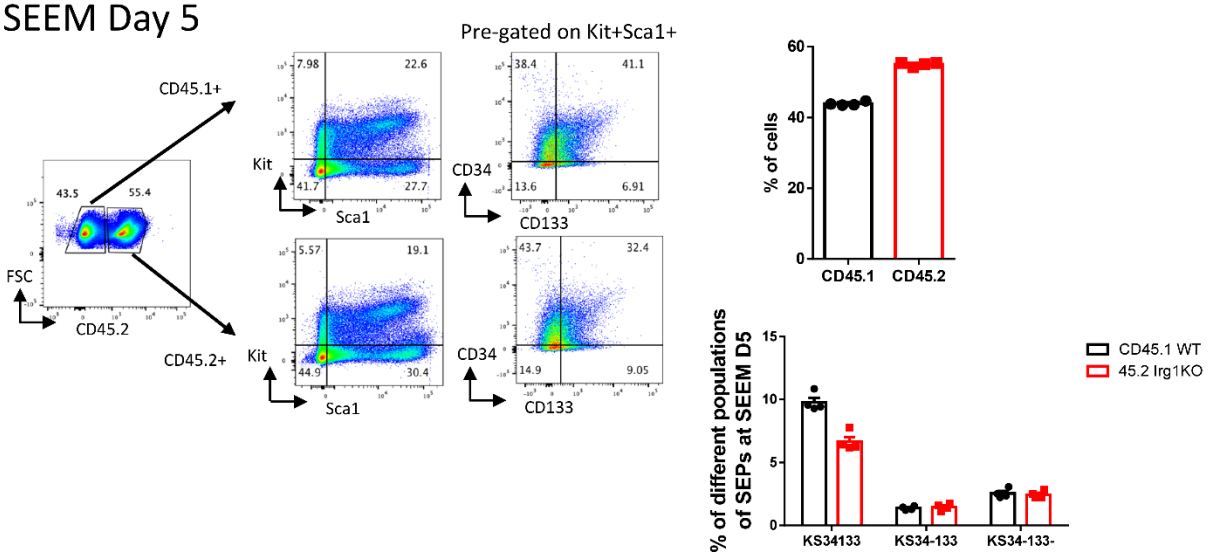

SEDM Day 3

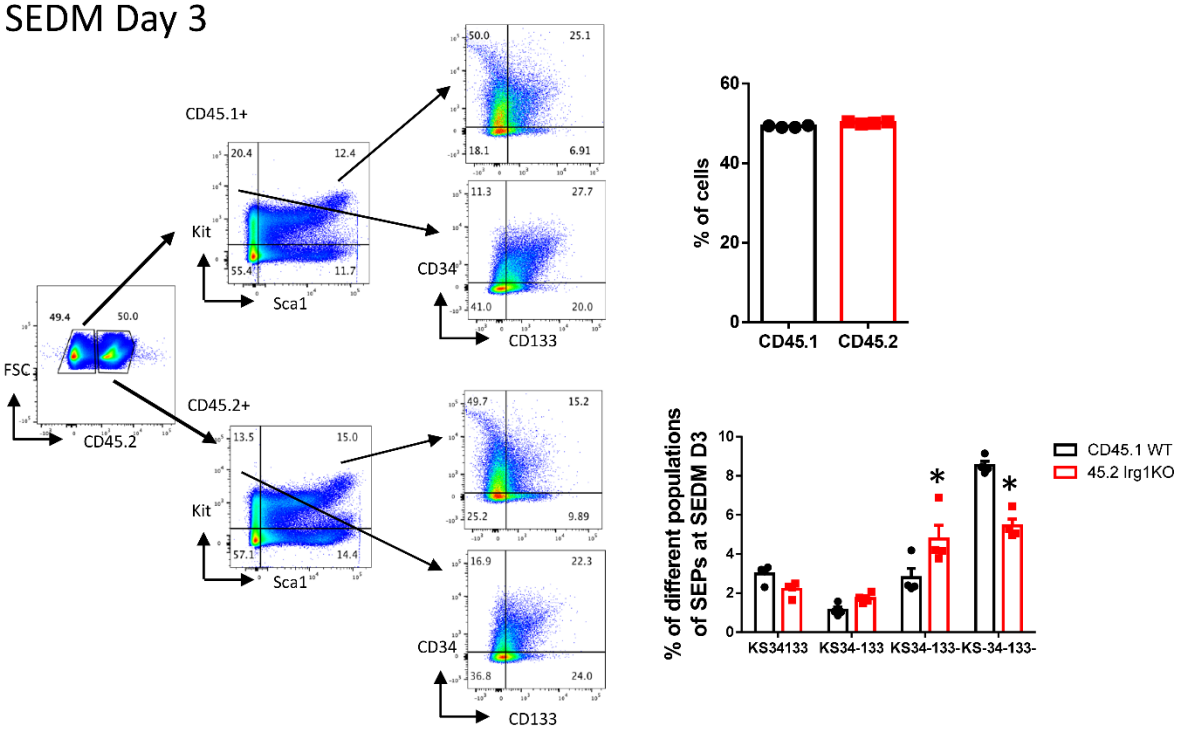

116

117

118

119

120

121 **Supplemental Figure 1.**

122 (A) Western blot analysis of Irg1 expression in Kit+ selected SEPs or stromal cells on days 3
123 and 5 of SEEM culture and days 1 and 3 of SEDM culture. Blots were probed with anti-β-actin
124 as a loading control. (B). Gating strategy showing flow cytometry analysis of proliferating SEPs.
125 Cells were stained for viability followed by gating on Kit and Sca1. Pre-gated Kit+Sca1+ cells
126 were then gated on CD34 and CD133 for analysis of different subpopulations. The identification
127 of CD34-CD133-Kit+Sca1+ as rapidly proliferating SEPs and CD34+CD133+Kit+Sca1+ cells as
128 slower proliferating cells comes from references [1, 6, 7].

129 (C) SEPs were treated ± 125 μM OI at SEEM day 3 for 24 hours (day 4) or 48 hrs (day 5).
130 Quantification of Nos2+ Kit+Sca1+ SEPs was determined by flow cytometry. (n=3 per group,
131 paired t test).

132 (D) CD45.2+;Irg1-/- and CD45.1+Irg1+/+ bone marrow cells were mixed at a 50:50 ratio and
133 cultured in SEEM for 5 days (top) or SEEM for 5 days and then switched to SEDM for 3 days
134 (bottom). Analysis of development of CD45.2+ mutant SEPs relative to CD45.1+ wildtype SEP
135 populations was determined by flow cytometry. Representative flow panels are shown on the
136 left, while quantification of the populations is shown on the right. (n=4, unpaired t-test) *$p<0.05$.

137

Figure S2

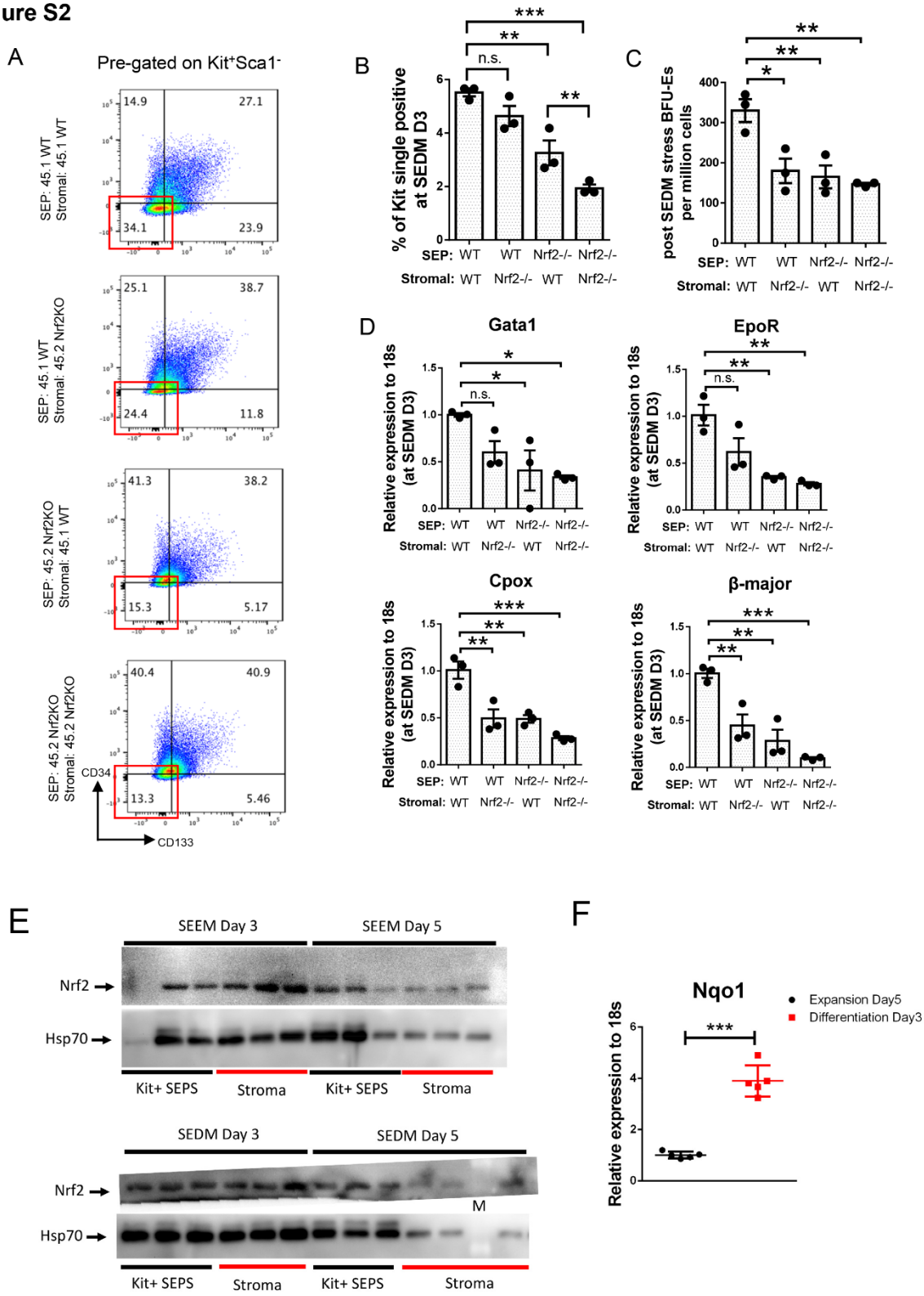

138

Supplemental Figure 2 continued

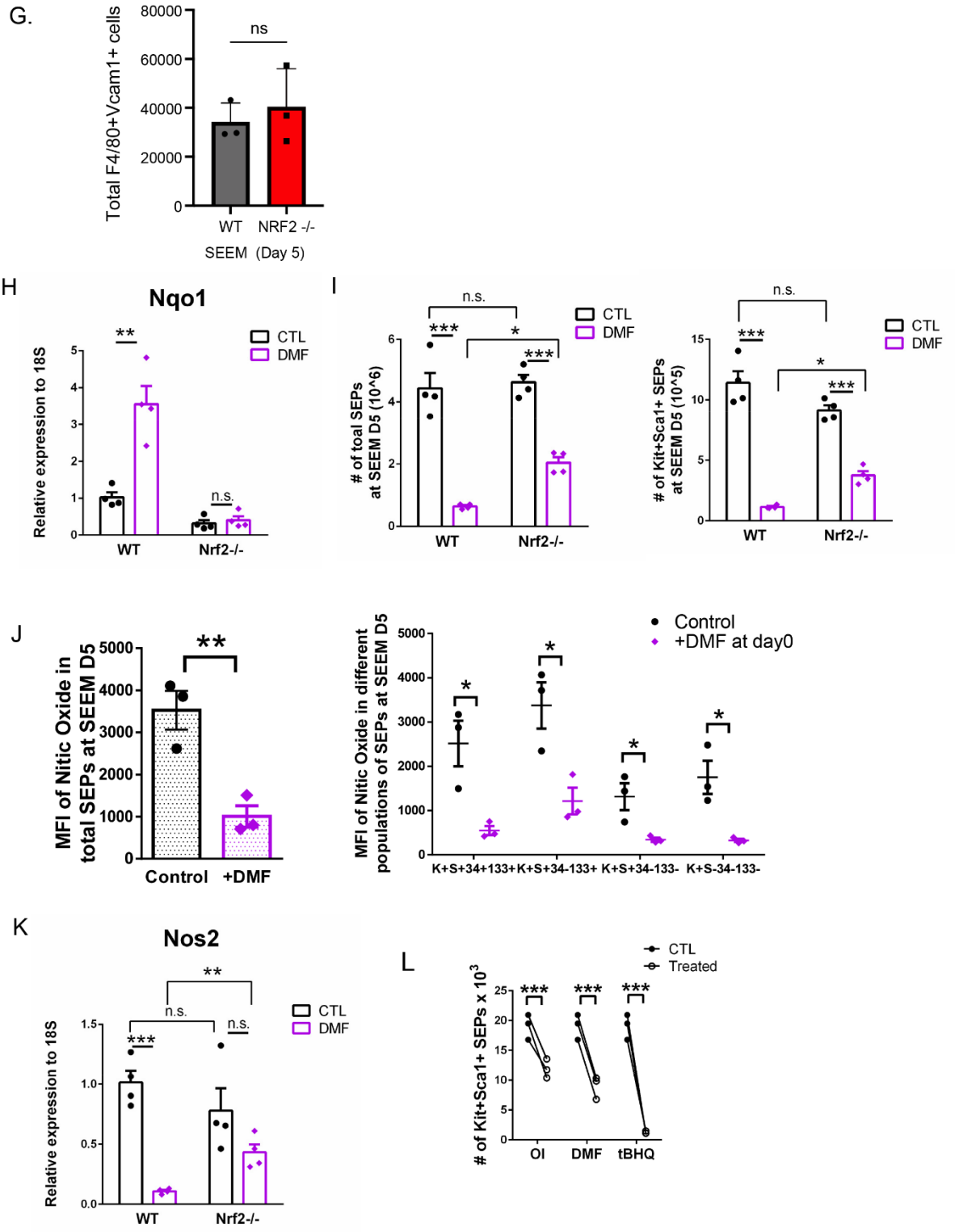

139

140 **Supplemental Figure 2. DMF impairs SEP expansion in a Nrf2-dependent manner.**

141 (A-D) WT (CD45.1) and Nrf2-/- (CD45.2) BM cells were cultured in SEEM for 5 days followed by
142 3 days in SEDM. When switched to SEDM, nonadherent SEPs were collected and plated on the
143 stromal layer from indicated genotypes.

144 (A) SEPs were isolated from SEDM cultures for flow cytometry analysis. CD45.1 was stained to
145 gate SEPs that were derived from the seeded non-adherent cells (Nrf2-/- CD45.2; WT CD45.1),
146 followed by gating on Kit and Sca1. Pre-gated Kit+Sca1- cells were next gated on CD34 and
147 CD133. Representative flow cytometry plots are shown. (B) Quantification of the percentages of
148 Kit+Sca1-CD34-CD133- SEPs from A (n=3 per group, one-way ANOVA/Tukey's).

149 (C) Analysis of the frequency of stress BFU-E colony formation (n=3 per group, one-way
150 ANOVA/Tukey's).

151 (D) qRT-PCR analysis of mRNA expression of indicated erythroid-specific genes (n=3 per
152 group, one-way ANOVA/Tukey's). Data represent mean ± SEM. n.s. $p > 0.05$, * $p < 0.05$, ** $p <$
153 0.01, *** $p < 0.001$.

154 (E). Western blot analysis of Nrf2 expression in Kit+SEPs and stromal cells on days 3 and 5 of
155 SEEM culture and days 3 and 5 Of SEDM culture. Hsp70 is used as a loading control. N=3 for
156 each time point.

157 (F). qRT-PCR analysis of Nqo1 expression in mRNA isolated form SEPs on day 5 of SEEM
158 (expansion) and Day 3 of SEDM (Differentiation) cultures. N=5 for each time point, unpaired t-
159 test.

160 (G). Flow cytometry analysis of F4/80+Vcam1+ cells in the stromal layer of wildtype control or
161 Nrf2-/- cultures on day 5 of SEEM culture. (n=3, unpaired t-test)

162 (H-I) WT and Nrf2-/- SEEM cultures were treated ± 30 μM DMF for 5 days. qRT-PCR analysis of
163 *Nqo1* expression (H), and analysis for numbers of total SEPs (left) and $Kit^{+}Sca1^{+}$ SEPs (right) (I)
164 (n=4; two-way ANOVA/Fisher's LSD).

165 (J) SEPs were treated ± 30 μM DMF at SEEM day 3 for 48 hrs. Quantification of intracellular NO
166 levels in total SEPs (left) and different SEP populations (right) by MFI of DAF-FM DA staining
167 (n=3 per group, unpaired t test).
168 (K) WT and Nrf2-/- SEEM cultures were treated ± 30 μM DMF for 5 days. qRT-PCR analysis of
169 *Nos2* expression (n=4; two-way ANOVA/Fisher's LSD).
170 (L) SEPs were treated with vehicle, 125 μM OI, 30 μM DMF or 20μM tBHQ at SEEM day 2 for
171 24 hrs, followed by flow cytometry analysis of numbers of $Kit^{+}Sca1^{+}$ SEPs (n=3 per group,
172 paired t test). Data represent mean ± SEM. n.s. $p > 0.05$, * $p < 0.05$, ** $p < 0.01$, *** $p < 0.001$.
173
174

Supplemental Figure 3

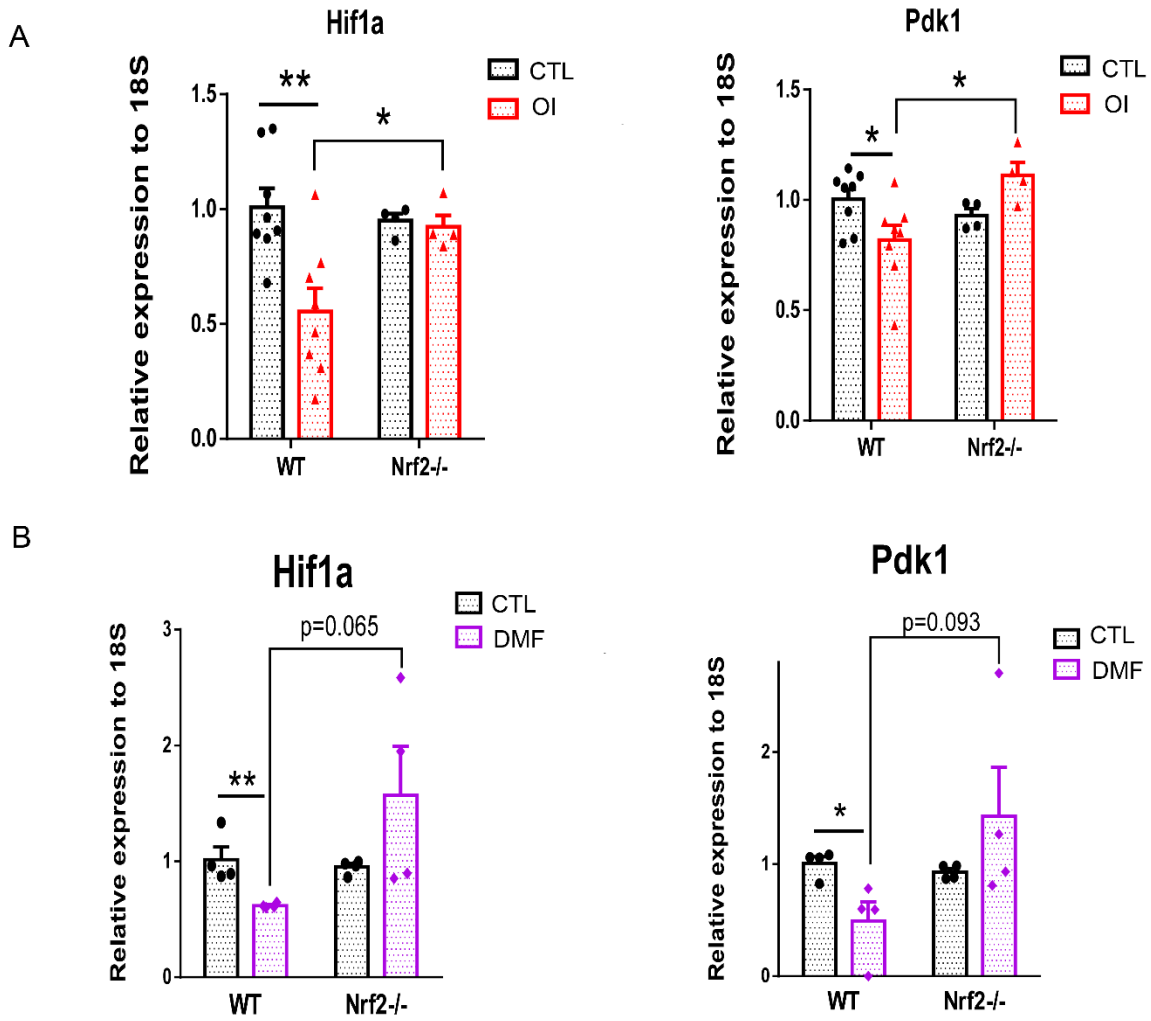

Supplemental Figure 3.

(A-B) WT and Nrf2-/- SEEM cultures were treated ± 125 μM OI for 5 days. The qRT-PCR analysis of *Hif-1α* (D) and *Pdk1* (E) expression (n=8 in WT and n=4 in Nrf2-/-; two-way ANOVA/Fisher's LSD).

(C-D) WT and Nrf2-/- SEEM cultures were treated ± 30 μM DMF for 5 days. The qRT-PCR analysis of *Hif-1α* (D) and *Pdk1* (E) expression (n=4; two-way ANOVA/Fisher's LSD).

Data represent mean ± SEM. * $p < 0.05$, ** $p < 0.01$.

184 Supplemental figure 4

A

Erythroid pathways

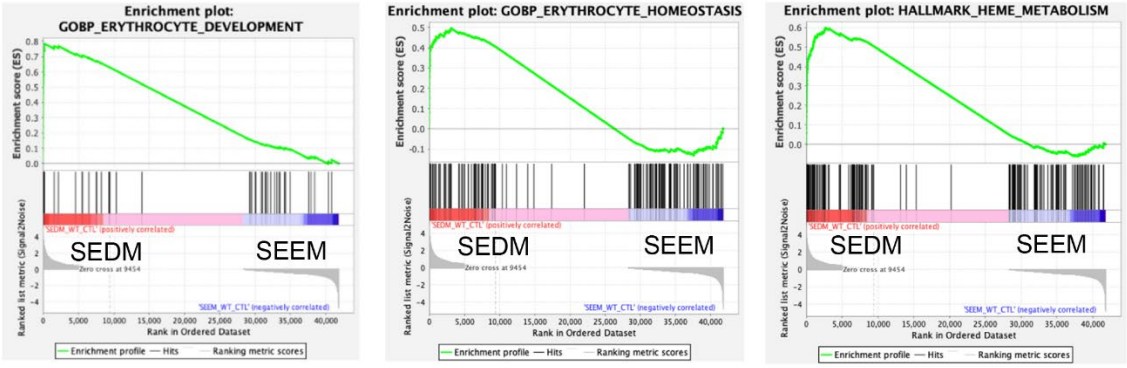

Pro-inflammatory pathways

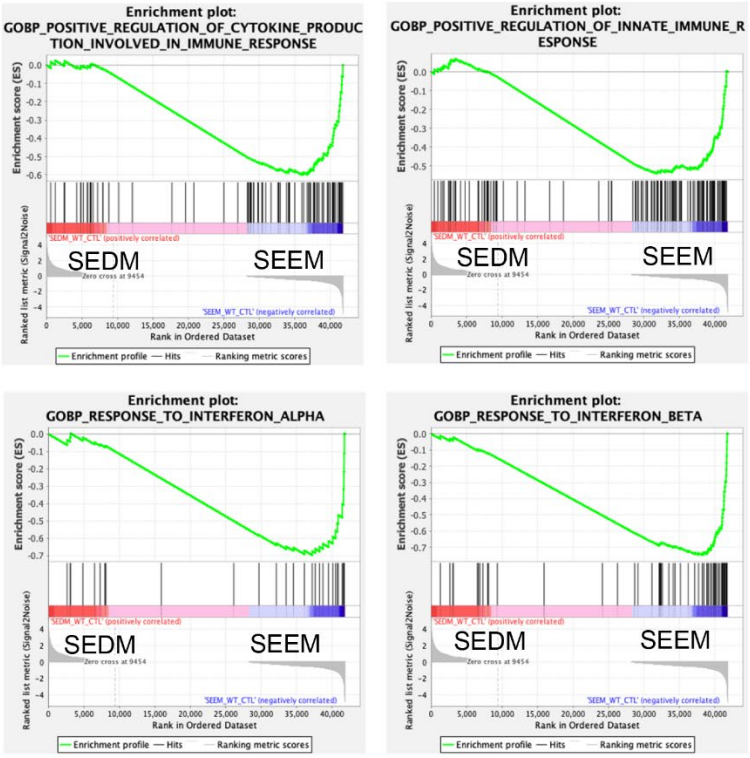

185

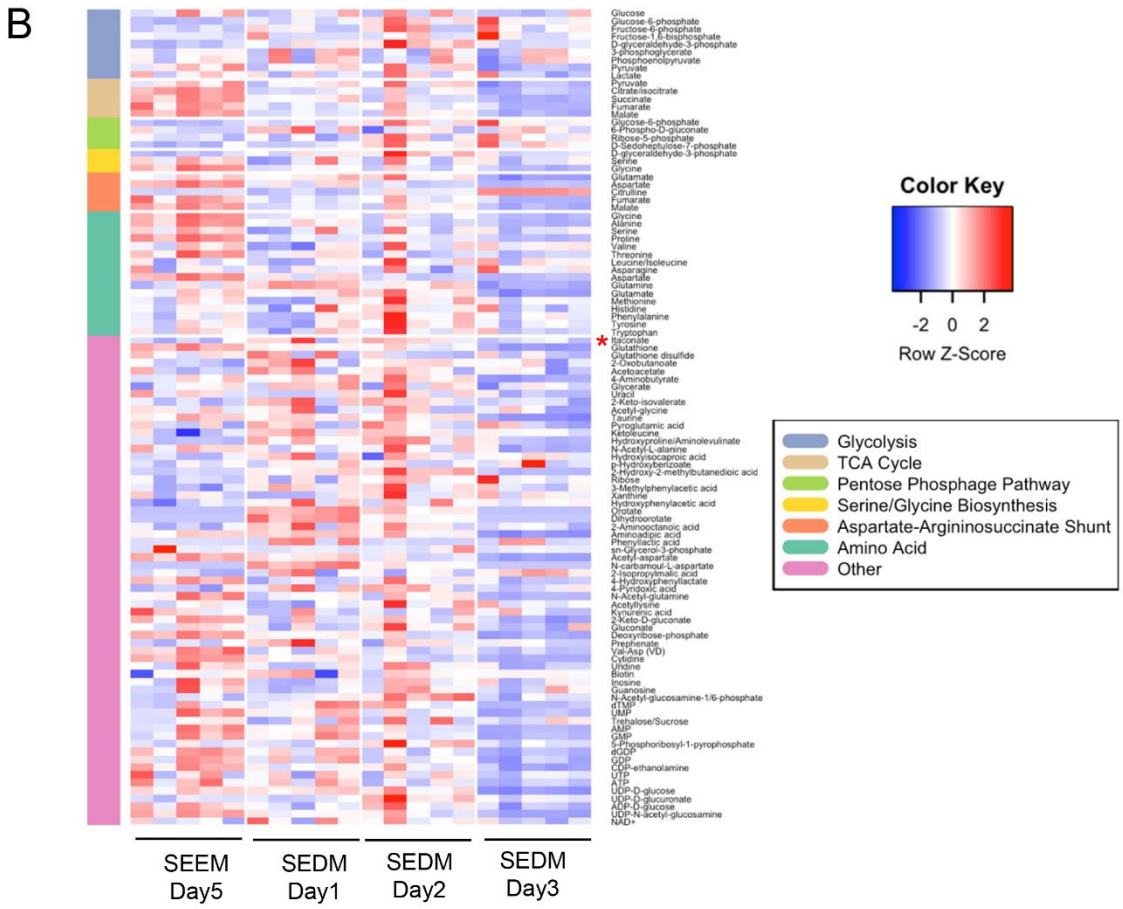

Supplemental Figure 4.

(A) GSEA analysis of RNA-seq data comparing SEPs from SEEM and SEDM cultures. (Top) Analysis of Erythrocyte development and homeostasis genes and Hallmark Heme biosynthesis pathways. (Bottom) Analysis of pro-inflammatory pathways. (B) SEPs were isolated from SEEM and SEDM cultures at indicated days for metabolomics analysis. A heatmap depicting the abundance of metabolites extracted from SEPs in selected pathways. Itaconate is highlighted by asterisk (*). Color represents row-wise scaled z-score of metabolite abundance (n=5 per time points).

Figure S5

A

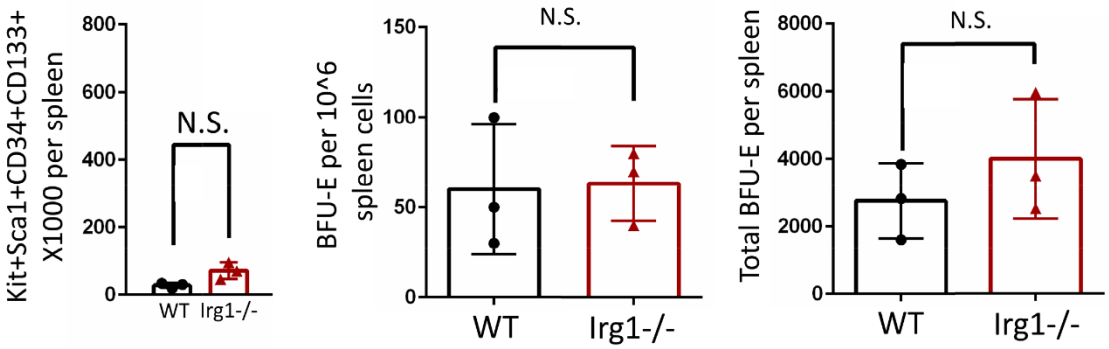

B

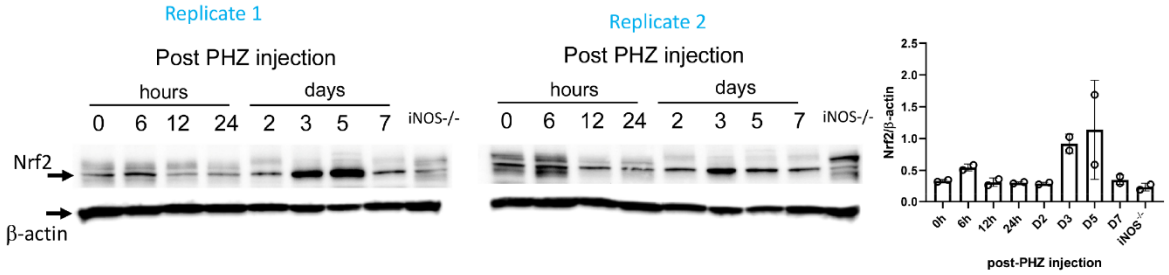

C

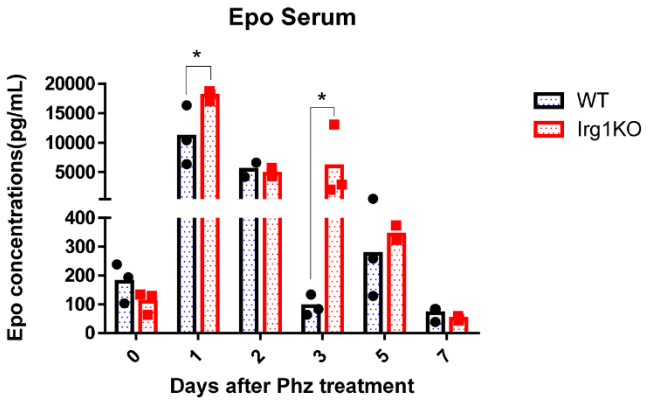

207 **Figure S5.**
208
209 (A) Analysis of CD34+CD133+Kit+Sca1+ SEPs and stress BFU-E in wildtype and Irg1-/-
210 spleens prior to treatment with HKBA. Total number of CD34+CD133+Kit+Sca1+ SEPs in the
211 spleen as analyzed by flow cytometry and total cellularity counts (left). Frequency of stress
212 BFU-E (middle) and total number of stress BFU-E(right) in the spleen prior to HKBA treatment
213 (n=3 per group).
214 (B). Western blot analysis of Nrf2 expression in spleen cells at the indicated time points after
215 PHZ treatment. β-actin is used as a loading control. Two replicates are shown. Quantification of
216 the bands using Image J software is shown to the right. Replicate 1 is shown in Figure 6A.
217 (C). ELISA analysis of Epo concentration in the serum of Irg1-/- or wildtype control mice on the
218 indicated days after PHZ treatment. (n=3 per time point, unpaired t-test). Data represent mean ±
219 SEM. N.S. $p > 0.05$, * $p < 0.05$, ** $p < 0.01$.
220
221

Figure S6

A

Downregulated in Nrf2KO

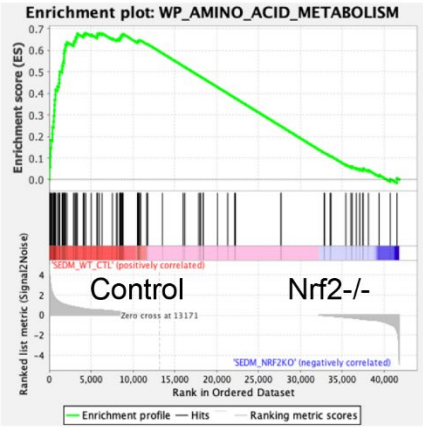

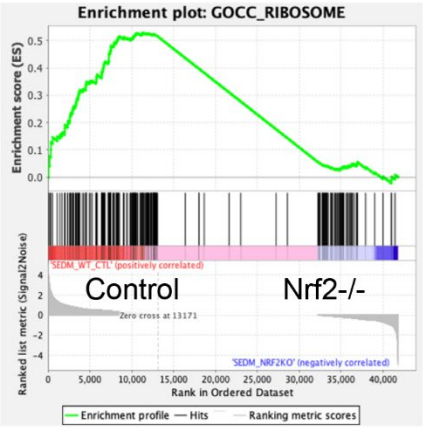

Figure S6.

(A). Gene set enrichment analysis of RNAseq data for SEPs day 3 of SEDM culture from control and Nrf2-/- cultures.

Supplemental data references

1. Xiang J, Wu DC, Chen Y, Paulson RF. In vitro culture of stress erythroid progenitors identifies distinct progenitor populations and analogous human progenitors. Blood. 2015;125(11):1803-12. Epub 2015/01/23. doi: 10.1182/blood-2014-07-591453. PubMed PMID: 25608563; PMCID: 4357585.

2. Bennett LF, Liao C, Paulson RF. Stress Erythropoiesis Model Systems. Methods Mol Biol. 2018;1698:91-102. Epub 2017/10/28. doi: 10.1007/978-1-4939-7428-3_5. PubMed PMID: 29076085; PMCID: PMC6510234.

3. Gardenghi S, Renaud TM, Meloni A, Casu C, Crielaard BJ, Bystrom LM, Greenberg-Kushnir N, Sasu BJ, Cooke KS, Rivella S. Distinct roles for hepcidin and interleukin-6 in the recovery from anemia in mice injected with heat-killed Brucella abortus. Blood. 2014;123(8):1137-45. Epub 2013/12/21. doi: 10.1182/blood-2013-08-521625. PubMed PMID: 24357729; PMCID: PMC3931188.

4. Mootha VK, Lindgren CM, Eriksson KF, Subramanian A, Sihag S, Lehar J, Puigserver P, Carlsson E, Ridderstråle M, Laurila E, Houstis N, Daly MJ, Patterson N, Mesirov JP, Golub TR, Tamayo P, Spiegelman B, Lander ES, Hirschhorn JN, Altshuler D, Groop LC. PGC-1alpha-responsive genes involved in oxidative phosphorylation are

247 coordinately downregulated in human diabetes. Nat Genet. 2003;34(3):267-73. Epub
248 2003/06/17. doi: 10.1038/ng1180. PubMed PMID: 12808457.
249
250 5. Subramanian A, Tamayo P, Mootha VK, Mukherjee S, Ebert BL, Gillette MA,
251 Paulovich A, Pomeroy SL, Golub TR, Lander ES, Mesirov JP. Gene set enrichment
252 analysis: a knowledge-based approach for interpreting genome-wide expression
253 profiles. Proc Natl Acad Sci U S A. 2005;102(43):15545-50. Epub 2005/10/04. doi:
254 10.1073/pnas.0506580102. PubMed PMID: 16199517; PMCID: PMC1239896.
255
256 6. Chen Y, Xiang J, Qian F, Diwakar BT, Ruan B, Hao S, Prabhu KS, Paulson RF.
257 Epo receptor signaling in macrophages alters the splenic niche to promote erythroid
258 differentiation. Blood. 2020;136(2):235-46. Epub 2020/05/01. doi:
259 10.1182/blood.2019003480. PubMed PMID: 32350523; PMCID: PMC7357191
260
261 7. Hao S, Xiang J, Wu DC, Fraser JW, Ruan B, Cai J, Patterson AD, Lai ZC,
262 Paulson RF. Gdf15 regulates murine stress erythroid progenitor proliferation and the
263 development of the stress erythropoiesis niche. Blood Adv. 2019;3(14):2205-17. Epub
264 2019/07/22. doi: 10.1182/bloodadvances.2019000375. PubMed PMID: 31324641;
265 PMCID: PMC6650738 .
266

267